

Highlights

A story of viral co-infection, co-transmission and co-feeding in ticks: how to compute an invasion reproduction number

Giulia Belluccini, Qianying Lin, Bevelynn Williams, Yijun Lou, Zati Vatansever, Martín López-García, Grant Lythe, Thomas Leitner, Ethan Romero-Severson, Carmen Molina-París

- We introduce a mathematical model of a single vector-borne virus in a population of ticks and hosts, with three different transmission routes, and derive its basic reproduction number.
- We study the dynamics of two different co-circulating viruses, or viral strains, in a tick population making use of a classic co-infection model.
- After performing an invasion analysis, we compute the invasion reproduction number, explain the issue of its non-neutrality, and propose five neutral alternatives.
- We conclude the paper with a summary of our proposals, their applicability and limitations.

A story of viral co-infection, co-transmission and co-feeding in ticks: how to compute an invasion reproduction number

Giulia Belluccini^{a,b}, Qianying Lin^a, Bevelynn Williams^b, Yijun Lou^c, Zati Vatansever^d, Martín López-García^b, Grant Lythe^b, Thomas Leitner^a, Ethan Romero-Severson^a, Carmen Molina-París^a

^a*T-6, Theoretical Biology and Biophysics, Los Alamos National Laboratory, Los Alamos, 87545, NM, USA*

^b*School of Mathematics, University of Leeds, Leeds, LS2 9JT, UK*

^c*Department of Applied Mathematics, Hong Kong Polytechnic University, Hong Kong SAR, China*

^d*Department of Parasitology, Faculty of Veterinary Medicine, Kafkas University, Kars, Turkey*

Abstract

With a single circulating vector-borne virus, the basic reproduction number incorporates contributions from tick-to-tick (co-feeding), tick-to-host and host-to-tick transmission routes. With two different circulating vector-borne viral strains, resident and invasive, and under the assumption that co-feeding is the only transmission route in a tick population, the invasion reproduction number depends on whether the model system of ordinary differential equations possesses the property of neutrality. We show that a simple model, with two populations of ticks infected with one strain, resident or invasive, and one population of co-infected ticks, does not have Alizon's neutrality property. We present model alternatives that are capable of representing the invasion potential of a novel strain by including populations of ticks dually infected with the same strain. The invasion reproduction number is analysed with the next-generation method and via numerical simulations.

Keywords: co-infection, co-transmission, co-feeding, invasion reproduction number, neutrality, mathematical model, basic reproduction number

PACS: 02.30.Hq, 87.10.Ed, 87.23.-n

2000 MSC: 37N25, 62P10

1. Introduction

Co-infection of a single host by at least two distinct viruses provides an opportunity for viruses to exchange genetic information through genomic reassortment or recombination [1, 2]. In fact, entirely novel pathogenic viruses have emerged from reassortment events of less pathogenic parents in nature [3–5]. Co-infection can be thought of as the rate-limiting step in the sudden emergence of genetically distant variants of existing human pathogens such as influenza, SARS-CoV-2, and Crimean Congo Hemorrhagic Fever Virus (CCHFV). Therefore, understanding the dynamics of co-infection in common host species, *e.g.*, arthropods (ticks or mosquitoes), is essential to study the emergence and re-emergence of both new and old human pathogens.

Genomic reassortment is possible in viruses with segmented genomes, such as the Bunyaviruses, which themselves include lethal pathogens of relevance to public health and of pandemic potential, *e.g.*, Lassa fever, Rift Valley fever and CCHF viruses [6]. Fig. 1 illustrates the dynamics of reassortment at the cellular level for Bunyaviruses, or more generally for a tri-segmented virus. CCHFV is a tick-borne Bunyavirus, with the potential to reassort, and an increasing geographical range due to the changing climate [7, 8]. Understanding how adaptable to different hosts this potentially fatal human pathogen is, what role co-infection (as a first step to genomic reassortment) will play in the generation of potential new viral strains, and how those variants will spread among already infected ticks, is a challenge for theoretical biology.

Due to the ability of ticks to carry multiple viruses or viral strains, epidemiologists have considered co-infection in tick-borne diseases [9–17], super-infection [9], and co-transmission [18–20]. Specifically, epidemiologists are interested in quantifying (or understanding) the invasion potential of a novel virus or strain [21, 22], given the endemic ability of a resident one [23]. In the same way as R_0 provides conditions for successful establishment of a single virus in a susceptible population, the *invasion reproduction number*, R_I , lends threshold conditions for successful invasion of a second virus when the population is endemic with the first one [24, 25]. For instance, Gao *et al.* developed a Susceptible-Infected-Susceptible (SIS) model for tick and host populations, and conducted a systematic analysis of invasion by the second virus [18]. More recently, Bushman and Antia have developed a general framework of the interaction between viral strains at the within-host level [26]. Pfab *et al.* have extended the time-since-infection framework of Kermack and McK-

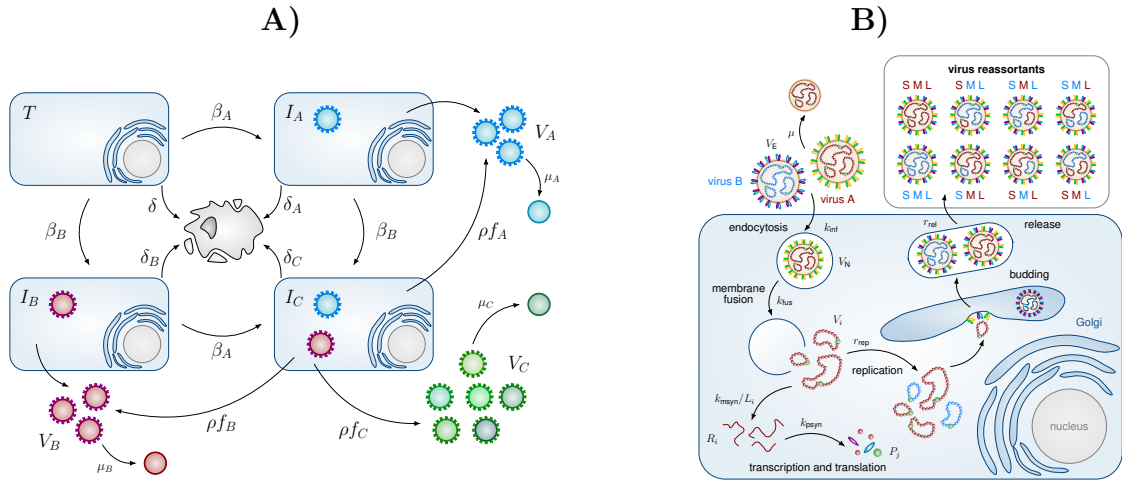


Figure 1: A) If two viral strains, V_A and V_B , are co-circulating, the target cells, T , of an infected host will become singly infected (I_A and I_B), and potentially co-infected (I_C). Co-infected cells have the potential to generate new viral progeny, different from that of the parental strains: $V_C \neq V_A$ and $V_C \neq V_B$. B) A co-infected cell can lead to reassortment events, and produce up to 2^3 different reassortants.

endrick [27] for two pathogens [28]. Rovenolt and Tate [29] have developed a model of co-infection to study how within-host interactions between parasites can alter host competition in an epidemic setting. Thao Le *et al.* [30] have studied a two-strain SIS model with co-infection (or co-colonisation) which incorporates variation in transmissibility, duration of carriage, pair-wise susceptibility to co-infection, co-infection duration, and transmission priority effects. Finally, Saad-Roy *et al.* [31] have considered super-infection and its role during the the first stage of an infection on the evolutionary dynamics of the degree to which the host is asymptomatic.

In the case of plant pathogens, recent experimental studies have shown the complex nature of vector-virus-plant interactions and their role in the transmission and replication of viruses as single and co-infections [32]. Allen *et al.* modeled the transmission dynamics of viruses between vectors and plants, under the assumption that co-infection could only take place in plants [24]. Chapwanya *et al.* developed a general deterministic epidemic model of crop-vector-borne disease for synergistic co-infection [33]. Miller *et al.* have shown that mathematical models on the kinetics of co-infection of plant cells with two strains could not adequately describe the data [34].

Current mathematical models of co-infection need to be put in perspective, as previously discussed by Lipsitch *et al.* and Alizon [35, 36]. Alizon compared different models of co-infection and raised an issue of *non-neutrality* [36]. He noticed that certain models of co-infection lead to an invasion reproduction number which does not tend to one, in the limit when the invasive and the resident pathogens are the same. To solve this problem, Alizon proposed an alternative model structure, which includes a population of dually infected individuals with the resident pathogen, to achieve the desired neutral invasion reproduction number [36, 37].

In this paper, we first present a mathematical model of a single vector-borne virus to understand the role that different transmission routes play in the dynamics of the infected populations. Then, we study the dynamics of two different viruses, or viral strains, in a tick population making use of a classic co-infection model. After performing an invasion analysis, we explain the issue of non-neutrality of the invasion reproduction number, and propose five neutral alternatives. We conclude the paper with a summary of our alternative proposals, their applicability and limitations.

2. Mathematical model of a single viral strain in a population of ticks and their vertebrate hosts

We consider a tick population feeding on a population of vertebrate hosts, where both populations are susceptible to infection with virus V_1 . The host and tick populations are divided into susceptible and infected subsets. In what follows the number of susceptible hosts (ticks) is denoted n_0 (m_0), and the number of infected hosts (ticks) is denoted n_1 (m_1), respectively.

The mathematical model considers immigration, death, viral transmission and recovery events in the populations; namely, susceptible hosts and ticks immigrate into the population with rate Φ_H and Φ_T , respectively. Susceptible and infected hosts can die with per capita rates μ_0 and μ_1 , respectively, whereas susceptible and infected ticks are characterised by the per capita death rates ν_0 and ν_1 , respectively. We assume an infected host can infect a susceptible tick with rate γ_1 , and an infected tick can infect a susceptible host with rate β_1 . Both of these transmission events involve a tick feeding on a vertebrate host, and are referred to as *systemic* transmission events [38]. The virus can additionally be transmitted from an infected tick to a susceptible one via co-feeding [39, 40]. This occurs when ticks feed on a host in clusters, and close to each other; that is, on the same host and at the same time. In

this instance the virus is transmitted by infected tick saliva, with this route of transmission referred to as *non-systemic* [38]. We denote by α_1 the rate at which an infected tick can infect a susceptible one via co-feeding. We assume that transmission events follow mass action kinetics. For example, in the case of co-feeding, and with m_0 and m_1 the number of susceptible and infected ticks, respectively, the rate of infection for the susceptible population is $\alpha_1 m_0 m_1$. Finally, once a tick contracts the virus, it remains infected for life [41]. On the other hand, vertebrate hosts are characterised by short-lasting viremia [41, 42]. We, thus, assume that hosts clear the virus with rate φ_1 [43, 44]. The above set of events are brought together in the following system of ordinary differential equations (ODEs), which describe the dynamics of susceptible and infected hosts and ticks:

$$\begin{aligned}
\frac{dn_0}{dt} &= \Phi_H - \mu_0 n_0 - \beta_1 n_0 m_1 + \varphi_1 n_1, \\
\frac{dn_1}{dt} &= -\mu_1 n_1 + \beta_1 n_0 m_1 - \varphi_1 n_1, \\
\frac{dm_0}{dt} &= \Phi_T - \nu_0 m_0 - \gamma_1 m_0 n_1 - \alpha_1 m_0 m_1, \\
\frac{dm_1}{dt} &= -\nu_1 m_1 + \gamma_1 m_0 n_1 + \alpha_1 m_0 m_1.
\end{aligned} \tag{1}$$

We note that this system of ODEs (1) has a virus-free equilibrium (VFE), $(n_0^*, 0, m_0^*, 0)$, given by

$$n_0^* = \frac{\Phi_H}{\mu_0}, \quad m_0^* = \frac{\Phi_T}{\nu_0}. \tag{2}$$

2.1. Basic reproduction number

The basic reproduction number, R_0 , measures the mean number of new infections produced by an infected individual (during its lifetime) in a population at the virus-free equilibrium; that is, when the population is completely susceptible [45]. R_0 (for the mathematical model (1)) can be calculated making use of the next-generation matrix method [46] as follows. The sub-system of differential equations for (n_1, m_1) is linearised at the VFE, and its Jacobian, J , is then written as $J \equiv T + V$, with T the 2×2 matrix of transmission events which accounts for new infections in the susceptible population, and $V \equiv J - T$, the 2×2 matrix tracking the changes in the state of the infected populations [46]. The next-generation matrix is defined as $\mathbb{K} \equiv T(-V)^{-1}$,

and the basic reproduction number, R_0 , is given by the largest eigenvalue of \mathbb{K} [46]. For our system we have

$$J \equiv \begin{pmatrix} -\mu_1 - \varphi_1 & \beta_1 n_0^* \\ \gamma_1 m_0^* & -\nu_1 + \alpha_1 m_0^* \end{pmatrix}, \quad (3)$$

with

$$T \equiv \begin{pmatrix} 0 & \beta_1 n_0^* \\ \gamma_1 m_0^* & \alpha_1 m_0^* \end{pmatrix}, \quad \text{and} \quad V \equiv \begin{pmatrix} -\mu_1 - \varphi_1 & 0 \\ 0 & -\nu_1 \end{pmatrix}, \quad (4)$$

so that

$$\mathbb{K} \equiv \begin{pmatrix} 0 & \beta_1 n_0^*/\nu_1 \\ \gamma_1 m_0^*/(\mu_1 + \varphi_1) & \alpha_1 m_0^*/\nu_1 \end{pmatrix}, \quad (5)$$

which in turn implies

$$R_0 \equiv \frac{1}{2} \left[\frac{\alpha_1 m_0^*}{\nu_1} + \sqrt{\left(\frac{\alpha_1 m_0^*}{\nu_1} \right)^2 + 4 \frac{\beta_1 \gamma_1 m_0^* n_0^*}{\nu_1 (\mu_1 + \varphi_1)}} \right]. \quad (6)$$

If $R_0 < 1$, the VFE is stable, and if $R_0 > 1$, it is unstable. The basic reproduction number can be rewritten as

$$R_0 = \frac{1}{2} \left(R_{TT} + \sqrt{R_{TT}^2 + 4R_{TH}R_{HT}} \right), \quad (7)$$

where we have introduced the following type reproduction numbers [47]

$$R_{TT} = \alpha_1 \frac{\Phi_T}{\nu_0 \nu_1}, \quad R_{TH} = \beta_1 \frac{\Phi_H}{\mu_0 \nu_1}, \quad R_{HT} = \gamma_1 \frac{\Phi_T}{\nu_0 (\mu_1 + \varphi_1)},$$

which represent the contribution of each route of transmission, tick-to-tick, tick-to-host and host-to-tick, respectively, to the total number of new infections (of ticks and hosts) in the susceptible population. R_{TT} , R_{TH} , and R_{HT} correspond to the entries of the next-generation matrix \mathbb{K} (see Eq. (5)). $R_{HH} = 0$, since the virus cannot be directly transmitted from an infected host to a susceptible one. The expression of the basic reproduction number for a single virus (see Eq. (7)) clearly shows that co-feeding represents a singular route of transmission, compared to systemic routes. For example, β_1 (or γ_1) can be very large, but if γ_1 (or β_1) is negligible, the contribution

to R_0 of viral systemic transmission will be negligible. Therefore, co-feeding events (as characterised by the parameter α_1), might maintain an epidemic if $R_{TT} > 1$. On the other hand, systemic transmission requires both tick-to-host and host-to-tick transmission routes to be non-vanishing, so that there is a chance for $R_0 > 1$, since as soon as either β_1 or γ_1 are equal to zero, $R_0 = 0$ in the absence of co-feeding.

We conclude this section mentioning a novel network approach (developed in Ref. [48]), to compute the parameters α_1 , β_1 , and γ_1 from first principles. It is reassuring to note that this approach leads to a next-generation matrix with the same structure as \mathbb{K} in Eq. (5).

2.2. Parameter values

We make use of recent literature to obtain parameter values for the ODE system (1). Table 1 contains a description of each model parameter, together with its plausible ranges and units. Since infection with CCHFV [42, 49] or *Borrelia* [48] is asymptomatic in ticks and vertebrate hosts (but unfortunately not in humans), we assume it does not affect their death rates; that is, $\mu_0 = \mu_1 \equiv \mu$ and $\nu_0 = \nu_1 \equiv \nu$ [18]. Given the narrow ranges in Table 1 for Φ_H , Φ_T , φ_1 and μ , we fix these parameters as follows: $\Phi_H = 1$ host per day, $\Phi_T = 2$ ticks per day, $\varphi_1 = 1/6$ per day, and $\mu = 10^{-3}$ per day. We derive plausible ranges for the other model parameters making use of Ref. [48], as illustrated in detail in Appendix A.

2.3. Visualization of the basic reproduction number

We illustrate the dependence of R_0 on the transmission parameters α_1 , β_1 and γ_1 , Fig. 2, making use of (6), and the parameter values from Section 2.2. Lighter colours correspond to greater values of R_0 (scale on right). Black lines represent a basic reproduction number equal to its critical value of 1. We set Φ_H , Φ_T , φ_1 , and μ to the values specified in Section 2.2, and set $\nu = 10^{-2}$ per day (see Appendix A). We consider a different value of α_1 in each panel: on the left, $\alpha_1 = 10^{-6}$, in the middle $\alpha_1 = 2 \times 10^{-5}$, and on the right $\alpha_1 = 10^{-4}$ (units as provided in Table 1). The corresponding values of R_{TT} are $R_{TT} = 1.2 \times 10^{-2}$, $R_{TT} = 0.4$, and $R_{TT} = 2$. Along the x -axis and y -axis we vary γ_1 and β_1 , respectively, from 0 to their maximum value listed in Table 1. We note that the area under the curve $R_0 = 1$ becomes smaller as α_1 increases (from left to right), until it becomes zero when co-feeding transmission contributes to make R_0 greater than one on its own. As one would expect, smaller values of the transmission parameters α_1 , β_1 and

Parameter	Event	Range	Units	Reference
β_1	$H_0 + T_1 \rightarrow H_1 + T_1$	$[10^{-7}, 10^{-5}]$	1/day/tick	[48]
γ_1	$T_0 + H_1 \rightarrow T_1 + H_1$	$[10^{-5}, 10^{-2}]$	1/day/host	[48]
α_1	$T_0 + T_1 \rightarrow T_1 + T_1$	$[10^{-6}, 10^{-4}]$	1/day/tick	[48]
ν_0	Death rate of T_0	10^{-2}	1/day	[48]
ν_1	Death rate of T_1	10^{-2}	1/day	[48]
μ_0	Death rate of H_0	$[2.8 \times 10^{-4}, 2.8 \times 10^{-3}]$	1/day	[50]
μ_1	Death rate of H_1	$[2.8 \times 10^{-4}, 2.8 \times 10^{-3}]$	1/day	[50]
Φ_T	Arrival of ticks	[0.5, 3.5]	tick/day	[38]
Φ_H	Arrival of hosts	[0.5, 1.5]	host/day	[38]
φ_1	$H_1 \rightarrow H_0$	[1/7, 1/5]	1/day	[44]
α_2	$T_0 + T_2 \rightarrow T_2 + T_2$	$[10^{-6}, 10^{-4}]$	1/day/tick	[48]
δ_1	Transmission of V_1 by T_c	$[10^{-6}, 10^{-4}]$	1/day/tick	Assumed
δ_2	Transmission of V_2 by T_c	$[10^{-6}, 10^{-4}]$	1/day/tick	Assumed
κ_1	Transmission of one copy of V_1 from M_1	$[10^{-6}, 10^{-4}]$	1/day/tick	Assumed
κ_2	Transmission of one copy of V_2 from M_2	$[10^{-6}, 10^{-4}]$	1/day/tick	Assumed
ϵ_c	Probability of co-transmission	[0, 1]	-	-
ϵ_1	Probability of dual transmission of V_1	[0, 1]	-	-
ϵ_2	Probability of dual transmission of V_2	[0, 1]	-	-
ν_2	Death rate of T_2	10^{-2}	1/day	[48]
ν_c	Death rate of T_c	10^{-2}	1/day	[48]

Table 1: Model parameters introduced in (1) (top half), and (8), (12), (13), and (15) (bottom half).

γ_1 correspond to lower values of R_0 (purple regions on the left and middle panels). Finally, we also note the symmetric role of β_1 and γ_1 in R_0 , as shown in (6).

3. Two viral strains: tick population and co-feeding transmission

In the previous section, we have shown that co-feeding can sustain an infection among ticks without systemic transmission. The remainder of the paper will focus on the co-feeding route of transmission. We now move to the more complex case where multiple viral strains co-exist, introducing the notions of co-infection and co-transmission. The population of ticks can be infected by two different circulating viral strains, V_1 and V_2 . V_1 is considered to be the resident strain and V_2 the invasive one (*e.g.*, one that emerges once the tick population is endemic with V_1). The population of ticks can be classified by its infection status in four different compartments, as susceptible and infected ticks with the resident strain, m_0 and m_1 , respectively, and infected ticks with the invasive strain and co-infected (*i.e.*, infected with both strains V_1 and V_2) ticks, m_2 and m_c , respectively. Figure 3a shows the mathematical model and the routes of viral transmission considered between

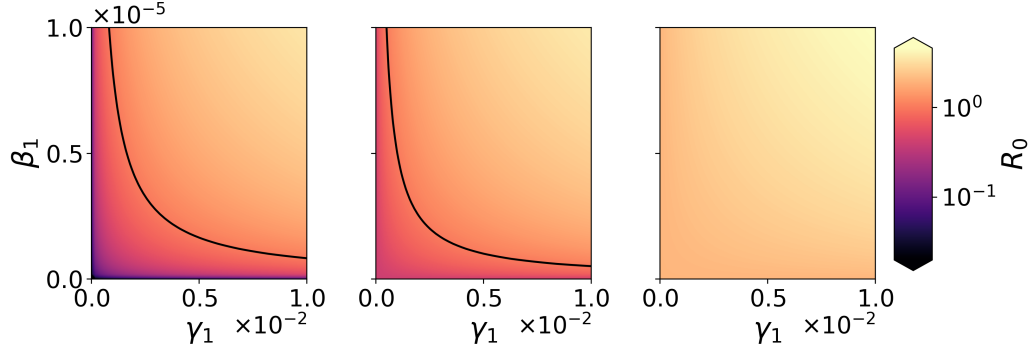


Figure 2: Contribution of α_1 , β_1 and γ_1 to the basic reproduction number, R_0 , given by Eq. (6). Model parameters have been chosen as discussed in Section 2.2 and units for α_1 , β_1 and γ_1 as in Table 1. On the left, $\alpha_1 = 10^{-6}$, in the middle $\alpha_1 = 2 \times 10^{-5}$, and on the right $\alpha_1 = 10^{-4}$. The parameters γ_1 and β_1 are varied along the x -axis and y -axis, respectively, from 0 to their maximum value listed in Table 1. Black curves represent the critical value $R_0 = 1$.

different tick compartments. The model corresponds to the following system of ODEs:

$$\begin{aligned}
\frac{dm_0}{dt} &= \Phi - \nu_0 m_0 - m_0(\lambda_1 + \lambda_2 + \lambda_c) , \\
\frac{dm_1}{dt} &= -\nu_1 m_1 + m_0 \lambda_1 - m_1(\lambda_2 + \lambda_c) , \\
\frac{dm_2}{dt} &= -\nu_2 m_2 + m_0 \lambda_2 - m_2(\lambda_1 + \lambda_c) , \\
\frac{dm_c}{dt} &= -\nu_c m_c + m_0 \lambda_c + m_1(\lambda_2 + \lambda_c) + m_2(\lambda_1 + \lambda_c) ,
\end{aligned} \tag{8}$$

where we have introduced

$$\begin{aligned}
\lambda_1 &= \alpha_1 m_1 + \delta_1(1 - \epsilon_c)m_c , \\
\lambda_2 &= \alpha_2 m_2 + \delta_2(1 - \epsilon_c)m_c , \\
\lambda_c &= (\delta_1 + \delta_2)\epsilon_c m_c ,
\end{aligned} \tag{9}$$

with $\epsilon_c \in [0, 1]$ representing the probability of co-transmission (V_1 and V_2). We have assumed that the m_1 (m_2) population has transmission parameter α_1 (α_2) for V_1 (V_2), and the m_c (co-infected) population has transmission parameter δ_1 for V_1 and δ_2 for V_2 , respectively. We have also slightly abused notation by writing $\Phi_T = \Phi$.

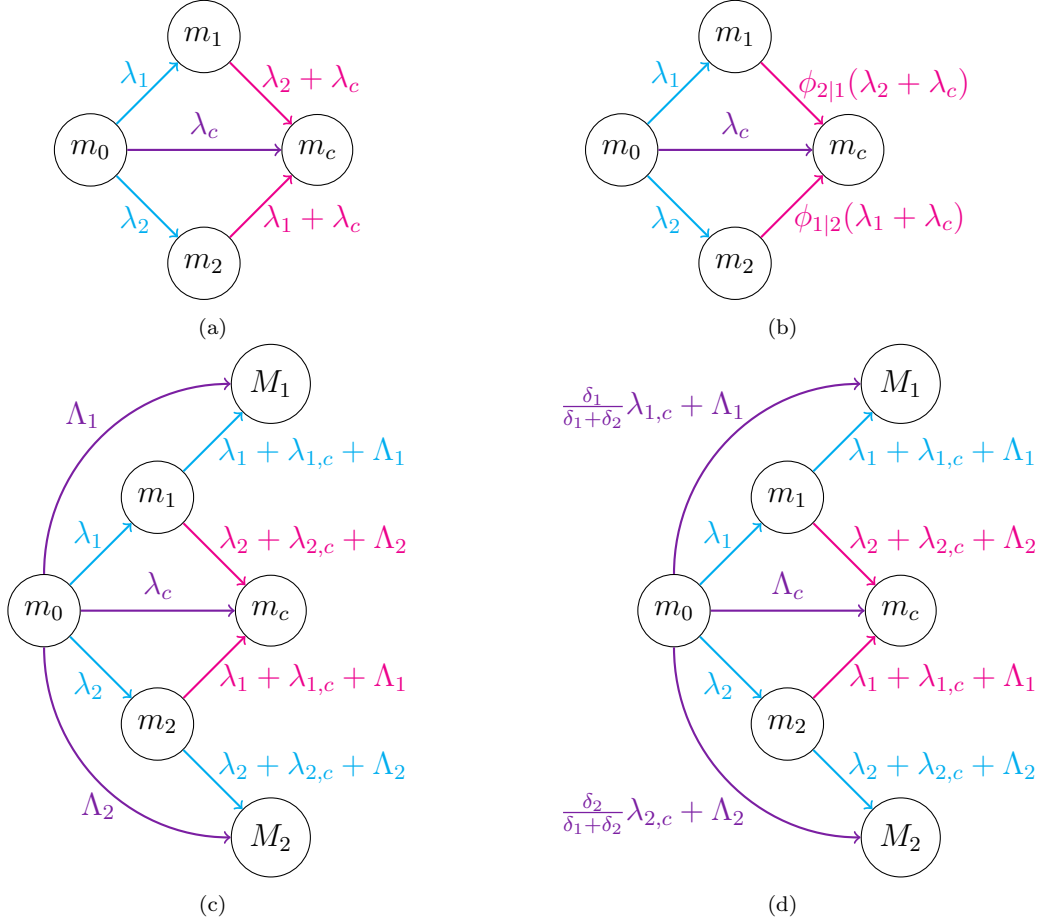


Figure 3: Illustrative diagrams of the mathematical models discussed in the paper for a population of co-feeding ticks with two viral strains. (a) Mathematical model of co-feeding transmission defined by Eq. (8). Transmission rates are defined in Eq. (9). (b) Within-host mathematical model of co-feeding transmission defined by Eq. (12). Transmission rates are defined in Eq. (9). (c) Alizon’s (generalised) proposal for co-infection and co-transmission described in Eq. (13). Transmission rates are defined in Eq. (14). (d) Two-slot mathematical model of co-infection and co-transmission defined in Eq. (15). Transmission rates are defined in Eq. (14) and Eq. (16).

3.1. Basic reproduction number

The mathematical model defined by the system of ODEs (8) has a virus-free equilibrium (VFE), $(m_0^*, 0, 0, 0)$, with $m_0^* = \frac{\Phi}{\nu_0}$. To compute its basic reproduction number, we make use of the next-generation matrix method, as illustrated in detail in Section 2.1. The T and V matrices are given by

$$T = \begin{pmatrix} \alpha_1 m_0^* & 0 & \delta_1(1 - \epsilon_c)m_0^* \\ 0 & \alpha_2 m_0^* & \delta_2(1 - \epsilon_c)m_0^* \\ 0 & 0 & (\delta_1 + \delta_2)\epsilon_c m_0^* \end{pmatrix}, \quad \text{and} \quad V = \begin{pmatrix} -\nu_1 & 0 & 0 \\ 0 & -\nu_2 & 0 \\ 0 & 0 & -\nu_c \end{pmatrix}.$$

Thus, by computing the eigenvalues of the next-generation matrix, $\mathbb{K} = T(-V)^{-1}$, the basic reproduction number of system (8) can be shown to be $R_0 = \max\{R_1, R_2, R_c\}$, with

$$R_1 = \frac{\alpha_1}{\nu_1} m_0^*, \quad R_2 = \frac{\alpha_2}{\nu_2} m_0^*, \quad R_c = \frac{(\delta_1 + \delta_2)\epsilon_c}{\nu_c} m_0^*.$$

Following the results from Ref. [18, Proposition 2.1], we can explore the boundary equilibria of system (8):

1. The virus-free equilibrium, $E_0 = (m_0^*, 0, 0, 0)$, always exists.
2. The endemic equilibrium with V_1 , $E_1 = \left(\frac{\nu_1}{\alpha_1}, \left(1 - \frac{1}{R_1}\right)\frac{\Phi}{\nu_1}, 0, 0\right)$, exists if and only if $R_1 > 1$.
3. The endemic equilibrium with V_2 , $E_2 = \left(\frac{\nu_2}{\alpha_2}, 0, \left(1 - \frac{1}{R_2}\right)\frac{\Phi}{\nu_2}, 0\right)$, exists if and only if $R_2 > 1$.
4. The endemic equilibrium with co-infected ticks, $E_c = \left(\frac{\nu_c}{(\delta_1 + \delta_2)\epsilon_c}, 0, 0, \left(1 - \frac{1}{R_c}\right)\frac{\Phi}{\nu_c}\right)$, exists if and only if $\epsilon_c = 1$, and $R_c > 1$.

3.2. Invasion reproduction number

We now assume that $R_1 > 1$, so that the endemic equilibrium E_1 of (8) exists. We write

$$\bar{m}_0 = \frac{\nu_1}{\alpha_1}, \quad \bar{m}_1 = \left(1 - \frac{1}{R_1}\right) \frac{\Phi}{\nu_1},$$

with $E_1 = (\bar{m}_0, \bar{m}_1, 0, 0)$. We aim to calculate the invasion reproduction number of V_2 by means of the next-generation matrix method. To this end, we identify the invasive sub-system of V_2 of Eq. (8), linearise it around E_1 ,

compute its Jacobian matrix, and define the 2×2 matrices T and V . We can write

$$T \equiv \begin{pmatrix} \alpha_2 \bar{m}_0 & \delta_2 (1 - \epsilon_c) \bar{m}_0 \\ \alpha_2 \bar{m}_1 & (\delta_1 + \delta_2) \epsilon_c (\bar{m}_0 + \bar{m}_1) + \delta_2 (1 - \epsilon_c) \bar{m}_1 \end{pmatrix}, \quad \text{and} \quad V \equiv \begin{pmatrix} -\alpha_1 \bar{m}_1 - \nu_2 & 0 \\ \alpha_1 \bar{m}_1 & -\nu_c \end{pmatrix}.$$

The next-generation matrix, $\mathbb{K} = T(-V)^{-1}$, is given by

$$\mathbb{K} \equiv \begin{pmatrix} R_{22} & R_{c2} \\ R_{2c} & R_{cc} \end{pmatrix},$$

with the type reproduction numbers R_{22} , R_{2c} , R_{c2} , and R_{cc} given by

$$\begin{aligned} R_{22} &= \frac{\alpha_2 \bar{m}_0}{\alpha_1 \bar{m}_1 + \nu_2} + \frac{\alpha_1 \bar{m}_1}{\alpha_1 \bar{m}_1 + \nu_2} \frac{\delta_2 (1 - \epsilon_c) \bar{m}_0}{\nu_c}, \\ R_{c2} &= \frac{\delta_2 (1 - \epsilon_c) \bar{m}_0}{\nu_c}, \\ R_{2c} &= \frac{\alpha_2 \bar{m}_1}{\alpha_1 \bar{m}_1 + \nu_2} + \frac{\alpha_1 \bar{m}_1}{\alpha_1 \bar{m}_1 + \nu_2} \frac{(\delta_1 + \delta_2) \epsilon_c (\bar{m}_0 + \bar{m}_1) + \delta_2 (1 - \epsilon_c) \bar{m}_1}{\nu_c}, \\ R_{cc} &= \frac{(\delta_1 + \delta_2) \epsilon_c (\bar{m}_0 + \bar{m}_1) + \delta_2 (1 - \epsilon_c) \bar{m}_1}{\nu_c}. \end{aligned}$$

The eigenvalues of \mathbb{K} are solutions of the following quadratic equation

$$\lambda^2 - (R_{22} + R_{cc})\lambda + (R_{22} R_{cc} - R_{c2} R_{2c}) = 0.$$

The invasion reproduction number, R_I , is the largest eigenvalue of \mathbb{K} , *i.e.*,

$$R_I = \frac{(R_{22} + R_{cc}) + \sqrt{(R_{22} + R_{cc})^2 - 4(R_{22} R_{cc} - R_{c2} R_{2c})}}{2}. \quad (10)$$

When $R_I > 1$, that is, $R_{22} + R_{cc} - R_{22} R_{cc} + R_{c2} R_{2c} > 1$, V_2 is able to invade a tick population where the resident strain V_1 is endemic.

4. Alternative neutral models of co-feeding, co-infection, and co-transmission

The invasion reproduction number of the mathematical model from Section 3.2 is not *neutral* [23, 37]. By neutrality, we mean the following: in the limit when the invasive strain tends to the resident one, there should be no

advantage for either strain, and thus, $R_I \rightarrow 1$. One can show for R_I given by Eq. (10) that $R_I \not\rightarrow 1$. In fact, we have $R_I \rightarrow 1$ iff $\delta_2 = \frac{\alpha_1}{1+R_1}$, and $R_I \rightarrow 1$ iff $\delta_2 + \delta_1 = \frac{\alpha_1}{R_1}$, for $\epsilon_c = 0$ and $\epsilon_c = 1$, respectively, under the assumption that infection does not affect the death rate, *i.e.*, $\nu_0 = \nu_1 = \nu_2 = \nu_c$. The issue of neutrality in co-infection models was brought up by Samuel Alizon in Ref. [37] and Lipsitch *et al.* in Ref. [35]. We now present five alternative *neutral* formulations of the previous model. The first (and less optimal) option for obtaining a neutral model is to force $R_I \rightarrow 1$ and in turn, consider the constraints this condition imposes on some of the model parameters. The second one, as proposed by us to Samuel Alizon in private communication, is to consider a normalised invasion reproduction number; that is, define $R_I^N = \frac{R_I}{\lim_{2 \rightarrow 1} R_I}$, where by $\lim_{2 \rightarrow 1} R_I$, we mean the value of the invasion reproduction number in the limit when the invasive strain tends to the resident one (see Section 4.1). The third one generalises the mathematical model (8) by introducing the idea of within-host probability of invasion (see Section 4.2). The fourth one, as proposed by Alizon [37], is to consider a more general class of models, with doubly infected individuals (see Section 4.3). A final one that we propose in Section 4.4, is a generalisation of the approach of Alizon [23, 37], which clearly articulates the issue of co-transmission.

4.1. A normalised invasion reproduction number

The invasion reproduction number given by Eq. (10) is not neutral. Let us then define a *normalised* invasion reproduction number, R_I^N , as follows

$$R_I^N = \frac{R_I}{\lim_{2 \rightarrow 1} R_I}, \quad (11)$$

where $\lim_{2 \rightarrow 1}$ means $\nu_2 \rightarrow \nu_1$, $\alpha_2 \rightarrow \alpha_1$, and $\delta_2 \rightarrow \delta_1$ for our co-infection model (see Eq. (8)). So defined, it is clear that $\lim_{2 \rightarrow 1} R_I^N = 1$, which is the desired neutrality condition. We note that the condition for the invasive strain to have the potential to become established is $R_I > 1$. Now that we have introduced a normalised invasion reproduction number, this condition becomes $R_I^N > (\lim_{2 \rightarrow 1} R_I)^{-1}$.

4.2. A model with within-host invasion

The fitness advantage of the invasive strain in model (8) stems from the assumption that V_2 can infect susceptible ticks and infected ticks by the resident strain with the same rate. However, this may not be realistic. For

instance, a small amount of transmitted (invasive) virus may be less likely to establish infection in a tick that already has a high resident viral load, compared to a fully susceptible tick. The probability of within-host invasion will, thus, depend on the relative within-host fitnesses of the invasive and resident strains. Therefore, we can adapt the previous model (Eq. (8)) by introducing the parameter $\phi_{i|j}$, which is the probability that strain i can establish co-infection in a tick already infected by strain j , given that there is transmission of strain i via co-feeding. This is similar to the super-infection framework described by Alizon in Ref. [36]. The model can then be described by the following system of ODEs:

$$\begin{aligned}
\frac{dm_0}{dt} &= \Phi - \nu_0 m_0 - m_0(\lambda_1 + \lambda_2 + \lambda_c) , \\
\frac{dm_1}{dt} &= -\nu_1 m_1 + m_0 \lambda_1 - m_1 \phi_{2|1}(\lambda_2 + \lambda_c) , \\
\frac{dm_2}{dt} &= -\nu_2 m_2 + m_0 \lambda_2 - m_2 \phi_{1|2}(\lambda_1 + \lambda_c) , \\
\frac{dm_c}{dt} &= -\nu_c m_c + m_0 \lambda_c + m_1 \phi_{2|1}(\lambda_2 + \lambda_c) + m_2 \phi_{1|2}(\lambda_1 + \lambda_c) ,
\end{aligned}
\tag{12}$$

where λ_1, λ_2 and λ_c are defined by Eq. (9). The transmission events of this model are summarised in Fig. 3b. In Appendix B we show that the invasion reproduction number for this model satisfies the desired neutrality condition.

4.3. A generalisation of Alizon's proposal

The mathematical model proposed by Alizon in Ref. [37] to obtain a neutral invasion reproduction number requires two additional populations (see Fig. 3c), namely the populations of doubly infected ticks with either V_1 or V_2 , denoted by M_1 and M_2 , respectively. Thus, there are six different tick compartments: m_0 , susceptible ticks, m_1, m_2 , ticks (singly) infected with either V_1 or V_2 , M_1, M_2 , doubly infected ticks with either V_1 or V_2 , and m_c , co-infected ticks with both V_1 and V_2 . We note that the co-infection models in Ref. [23] do not consider co-transmission, but it is discussed in Ref. [37]. Thus, in what follows, and to develop a mathematical model of co-infection and co-transmission in co-feeding ticks, we explain in detail what happens when a co-infected tick transmits virus to a singly infected tick. If co-transmission of both, resident and invasive, strains occurs, the singly infected tick can only acquire one new viral strain, since the mathematical model does not accommodate triply infected ticks. Therefore, if co-transmission

takes place, a singly infected tick will acquire V_1 with probability $\frac{\delta_1}{\delta_1 + \delta_2}$, or V_2 with probability $\frac{\delta_2}{\delta_1 + \delta_2}$. Hence, the overall rate at which a co-infected tick transmits V_1 to a singly infected tick is $(1 - \epsilon_c)\delta_1 + (\delta_1 + \delta_2)\epsilon_c\frac{\delta_1}{\delta_1 + \delta_2} = \delta_1$, where the first term represents transmission of V_1 if no co-transmission, and the second term represents transmission of V_1 in the event of co-transmission. Similarly, the overall rate a co-infected tick transmits V_2 to a singly infected tick is δ_2 . We now write down the system of ODEs for Alizon's generalised mathematical model of a co-feeding tick population, with two circulating viral strains, which allows for co-infection and co-transmission, and at most doubly infected ticks (with the same strain M_1 and M_2 , or with different ones m_c). We have

$$\begin{aligned}
\frac{dm_0}{dt} &= \Phi - \nu_0 m_0 - m_0 (\lambda_1 + \lambda_2 + \lambda_{1,c} + \lambda_{2,c} + \Lambda_1 + \Lambda_2), \\
\frac{dm_1}{dt} &= -\nu_1 m_1 + m_0 \lambda_1 - m_1 (\lambda_1 + \lambda_2 + \lambda_{1,c} + \lambda_{2,c} + \Lambda_1 + \Lambda_2), \\
\frac{dm_2}{dt} &= -\nu_2 m_2 + m_0 \lambda_2 - m_2 (\lambda_1 + \lambda_2 + \lambda_{1,c} + \lambda_{2,c} + \Lambda_1 + \Lambda_2), \\
\frac{dm_c}{dt} &= -\nu_c m_c + m_0 (\lambda_{1,c} + \lambda_{2,c}) + m_1 (\lambda_2 + \lambda_{2,c} + \Lambda_2) + m_2 (\lambda_1 + \lambda_{1,c} + \Lambda_1), \\
\frac{dM_1}{dt} &= -v_1 M_1 + m_0 \Lambda_1 + m_1 (\lambda_1 + \lambda_{1,c} + \Lambda_1), \\
\frac{dM_2}{dt} &= -v_2 M_2 + m_0 \Lambda_2 + m_2 (\lambda_2 + \lambda_{2,c} + \Lambda_2),
\end{aligned} \tag{13}$$

where we define

$$\begin{aligned}
\lambda_1 &= \alpha_1 m_1 + \delta_1 (1 - \epsilon_c) m_c + 2\kappa_1 (1 - \epsilon_1) M_1, \\
\lambda_2 &= \alpha_2 m_2 + \delta_2 (1 - \epsilon_c) m_c + 2\kappa_2 (1 - \epsilon_2) M_2, \\
\lambda_{1,c} &= \delta_1 \epsilon_c m_c, \\
\lambda_{2,c} &= \delta_2 \epsilon_c m_c, \\
\Lambda_1 &= 2\kappa_1 \epsilon_1 M_1, \\
\Lambda_2 &= 2\kappa_2 \epsilon_2 M_2,
\end{aligned} \tag{14}$$

with ϵ_c , the probability of co-transmission of the two viral strains by a co-infected (m_c) tick, and with ϵ_1 (ϵ_2) the probability of co-transmission by a doubly infected tick M_1 (M_2), respectively. The original model of co-infection

with co-transmission defined in Ref. [37] assumed $\epsilon_1 = \epsilon_2 = \epsilon_c = \epsilon$. We warn the reader that we have defined λ_1 and λ_2 to mean two different things in Eq. (14) and Eq. (9). We shall always clarify in what follows, which of the two definitions is implied. Fig. 3c shows the transmission events described by Eq. (13). We note that co-transmission by the M_1 tick population to a susceptible tick implies double transmission of the resident viral strain V_1 , and that co-transmission by the M_2 tick population (to a susceptible tick) implies double transmission of the resident strain V_2 . Finally, the parameter κ_1 (κ_2) is the rate of transmission of a single copy of V_1 (V_2) from an M_1 (M_2) tick to a susceptible one; thus, the factor of 2 in the previous expression for Λ_1 (Λ_2). We remind the reader that the model defined above includes death, immigration and transmission events. We have assumed each tick compartment has a different death rate, and immigration replenishes the susceptible tick compartment. In Appendix C we carefully derive the invasion reproduction number of this model and show its neutrality.

4.4. *Two-slot model of co-feeding, co-infection and co-transmission*

In the model defined by Eq. (13), a co-transmission event from a co-infected tick, in the m_c compartment, to a susceptible tick implies the transmission of both viral strains at once. Here we extend the previous model to allow for the possibility that such a co-transmission event could instead result in the transmission of two copies of V_1 or two copies of V_2 . The idea of this generalised *two-slot model* is as follows: since ticks can be at most doubly infected, we assume each tick has two *infection slots* that can be occupied (or not). In the previous model, “co-transmission” to a susceptible tick meant transmission of both viral strains. In this model “co-transmission” means occupying both slots, in such a way, that the slots can be occupied by two copies of the same virus (leading to M_1 or M_2 ticks), or two different strains

(leading to m_c ticks). The dynamics of the two-slot model can be written as

$$\begin{aligned}
\frac{dm_0}{dt} &= \Phi - \nu_0 m_0 - m_0(\lambda_1 + \lambda_2 + \lambda_{1,c} + \lambda_{2,c} + \Lambda_1 + \Lambda_2), \\
\frac{dm_1}{dt} &= -\nu_1 m_1 + m_0 \lambda_1 - m_1(\lambda_1 + \lambda_2 + \lambda_{1,c} + \lambda_{2,c} + \Lambda_1 + \Lambda_2), \\
\frac{dm_2}{dt} &= -\nu_2 m_2 + m_0 \lambda_2 - m_2(\lambda_1 + \lambda_2 + \lambda_{1,c} + \lambda_{2,c} + \Lambda_1 + \Lambda_2), \\
\frac{dm_c}{dt} &= -\nu_c m_c + m_0 \Lambda_c + m_1(\lambda_2 + \lambda_{2,c} + \Lambda_2) + m_2(\lambda_1 + \lambda_{1,c} + \Lambda_1), \\
\frac{dM_1}{dt} &= -v_1 M_1 + m_0 \left(\Lambda_1 + \frac{\delta_1}{\delta_1 + \delta_2} \lambda_{1,c} \right) + m_1(\lambda_1 + \lambda_{1,c} + \Lambda_1), \\
\frac{dM_2}{dt} &= -v_2 M_2 + m_0 \left(\Lambda_2 + \frac{\delta_2}{\delta_1 + \delta_2} \lambda_{2,c} \right) + m_2(\lambda_2 + \lambda_{2,c} + \Lambda_2),
\end{aligned} \tag{15}$$

where $\lambda_1, \lambda_2, \lambda_{1,c}, \lambda_{2,c}, \Lambda_1,$ and Λ_2 have been defined in Eq. (13), and with Λ_c given by

$$\Lambda_c = \frac{2\delta_1\delta_2}{\delta_1 + \delta_2} \epsilon_c m_c. \tag{16}$$

In Appendix D we describe in great detail the transmission events considered in the two-slot mathematical model, show the existence of an endemic equilibrium for V_1 , and prove that the model leads to a neutral invasion reproduction number.

4.5. Numerical study of the invasion reproduction number

In Section 3 we have defined and computed the invasion reproduction number for a mathematical model of co-infection and co-transmission in co-feeding ticks. We have argued that such a model is not neutral, and have in turn proposed different mathematical models which do not suffer from such problem. We now propose a numerical study of the invasion reproduction number for the “not-neutral” model introduced in Section 3, as well as the invasion reproduction number for the model solutions proposed above to guarantee neutrality.

In what follows we assume that $\kappa_1 = \alpha_1/2$, and $\kappa_2 = \alpha_2/2$, which are appropriate choices when considering viral infections or micro-parasites [37]. As discussed by Alizon in Ref. [37], if an infected host (by a certain viral strain) is re-infected by the exact same strain, we do not expect to see a change in its viral load (and hence in transmission rate). For co-infected ticks

in the m_c compartment (and infected by both V_1 and V_2), it is reasonable to hypothesise that potential within-tick interactions between the two strains do not lead to a change in transmission rates, when compared to doubly infected ticks in the M_1 or M_2 compartments. Thus, we assume $\delta_1 = \kappa_1$ and $\delta_2 = \kappa_2$. Finally, and as justified earlier, we set $\nu_0 = \nu_1 = \nu_2 = \nu_c = \nu_1 = \nu_2 = 10^{-2}$ per day. We also fix the immigration rate to be $\Phi = 2$ ticks per day, and $\alpha_1 = 10^{-4}$ per tick per day. These choices lead to a basic reproduction number of $R_1 = 2$ for the resident strain, V_1 .

In Fig. 4 we compare how different values of the transmission parameter, α_2 , and the co-transmission probability, ϵ_c , affect the invasion reproduction number, R_I , computed in the “not-neutral” scenario (10) (panel (a)), in the normalized proposal of Eq. (11) (panel (a^{*})), in the within-host model (12) (panel (b)), in Alizon’s model with co-transmission (13) (panel (c)), and in the two-slot mathematical model (15) (panel (d)). In particular, ϵ_c is varied along the x -axis, whereas the ratio α_2/α_1 is varied from 0.5 to 1.5 along the y -axis. Black lines mark the contours where the invasion reproduction number, R_I , is equal to 1. For Alizon’s model and the two-slot extension, we have set $\epsilon_1 = \epsilon_2 = 1/2$. For the within-host model, we define the probability that strain i can establish co-infection in a tick already infected by strain j as follows

$$\phi_{i|j} = \begin{cases} 1, & \text{if } \alpha_i > \alpha_j, \\ 0, & \text{if } \alpha_i \leq \alpha_j. \end{cases}$$

We note that the highest values of the invasion reproduction number occur in panel (a) and (b) of Fig. 4. In panel (a), the invasion reproduction number is clearly not neutral, since $R_I > 1$ when $\alpha_2 = \alpha_1$, and also for some regions of parameter space with $\alpha_2 < \alpha_1$. For this model, if infected ticks with the invasive strain, V_2 , are rare compared to ticks infected with the resident strain, V_1 , then V_2 has an initial advantage over V_1 . Each tick infected with the invasive strain has the opportunity to infect a much larger number of ticks ($\bar{m}_0 + \bar{m}_1$), than those which can be infected by a tick from the m_1 compartment. This allows V_2 to invade the V_1 endemic system, for large enough values of α_2 and ϵ_c . The co-transmission probability, ϵ_c , affects the value of R_I , since it changes the rate at which co-infected ticks transmit V_1 and V_2 to susceptible ticks, m_0 . These rates are $\delta_1 + \epsilon_c\delta_2$ and $\delta_2 + \epsilon_c\delta_1$, respectively. Therefore a higher probability of co-transmission enables both strains to be transmitted more often. For the normalised invasion reproduction number in panel (a^{*}), $R_I = 1$ when $\alpha_2 = \alpha_1$, for every value of ϵ_c , given its definition.

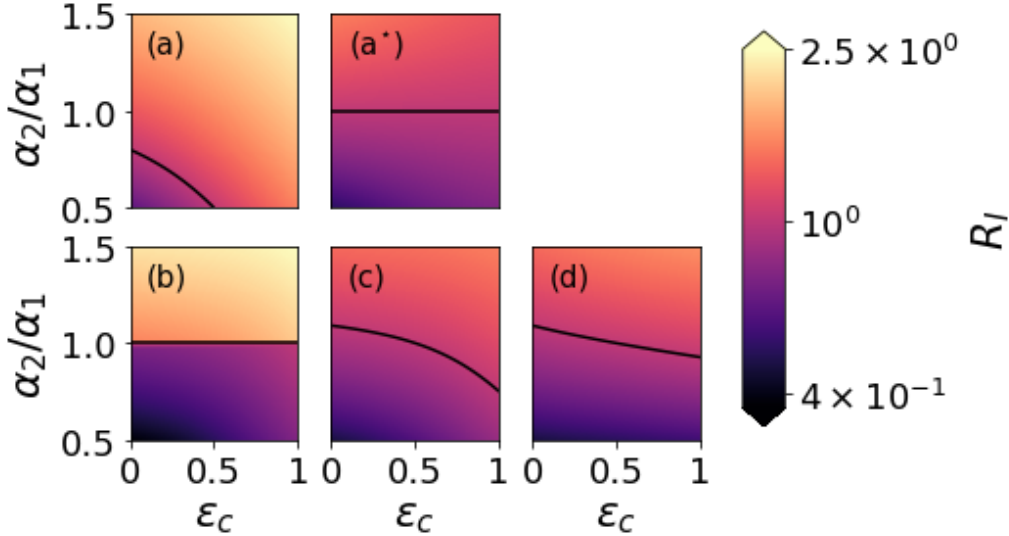


Figure 4: Heatmaps of the invasion reproduction number for (a) the “not-neutral” model (10), (a*) the normalised proposal (11), (b) the within-host model with ϕ_{ij} , Eq. (12), (c) Alizon’s model with co-transmission (13), and (d) the two-slot mathematical model (15). The x -axis represents ϵ_c , the probability of co-transmission from co-infected ticks. The y -axis shows the ratio α_2/α_1 in the range $[0.5, 1.5]$. We set $\alpha_1 = 10^{-4}$ per tick per day. Black lines mark the contours where the invasion reproduction number, R_I , is equal to 1. For Alizon’s model and the two-slot extension, we have set $\epsilon_1 = \epsilon_2 = 1/2$.

When $\alpha_2 \neq \alpha_1$, R_I does depend on ϵ_c , but less so than for the model of panel (a), since $\lim_{\epsilon_c \rightarrow 1} R_I$ increases with ϵ_c . In panel (c), showing the invasion reproduction number for Alizon’s model, when $\epsilon_c = 1/2$ (equal to ϵ_1 and ϵ_2), $R_I = 1$ for $\alpha_2 = \alpha_1$. As ϵ_c increases, so does the value of R_I , since a higher co-transmission probability enables V_2 to be transmitted along with V_1 more often. The invasion reproduction number of the two-slot model in panel (d) behaves in a similar fashion. However, increasing ϵ_c does not give as much of an advantage to the invasive strain, since co-transmission events can result in the transmission of two copies of V_1 .

5. Discussion and conclusions

In this paper, we consider the role of different transmission routes for a single vector-borne virus in a population of ticks and vertebrate hosts. We then study co-infection and co-transmission of two circulating vector-borne viral strains in a population of co-feeding ticks. We define and compute

both the basic reproduction number and the invasion reproduction number, which provides the conditions under which a new variant can emerge (possibly endogenously from genomic reassortment). We illustrate how a classic and *intuitive* model of invasion was not, in fact, neutral with respect to the invading strain; that is, using this model to understand, for example, the minimum selective advantage that needs to be present for an invading strain to take hold of an endemic population (with the resident one) will privilege one strain over the other. This is not a problem *per se*, as it might be the correct model from a mechanistic perspective. However, it is important to characterise the underlying properties of a mathematical model, especially if it is intended to be used as part of an inference procedure. We also presented several alternative formulations of co-infection and co-transmission models that are, by definition neutral. We have shown that each model has distinct and specific behaviour concerning the invasion reproduction number. The take-home message of this review is that the assumptions used to model these important and complex infection systems matter, specially when making inferences about pathogens of potential pandemic emergence. In the real world, the choice of model, from the different alternatives presented and discussed here, will clearly depend on the virus, as well as the immunology and ecology of the hosts those viruses infect.

In conclusion, we note that while we have focused on deterministic models of tick-borne disease transmission, stochastic analogous may be considered instead, particularly when studying the invasion potential of a rare circulating viral strain [15, 51, 52]. In a stochastic framework, the reproduction number is defined as a random variable rather than as an average [53], since its distribution encodes the probability of an epidemic occurring if a pathogen is introduced into a fully susceptible population by a small number of infected individuals [53]. Thus, future work should include a study of the invasion reproduction number probability distribution, as well as an exploration of the issue of non-neutrality making use of stochastic approaches [54]. Finally, given recent reports which indicate an increase in the number of Zika and Dengue virus co-infection cases in expanding co-endemic regions [55], it is of utmost importance to have suitable within-host mathematical models to study the impact of co-infection on viral infection dynamics.

Appendix A. Parameters from network approach

Since CCHFV infection is asymptomatic in ticks and vertebrate hosts, we assume that it does not affect their death rates; that is, $\mu_0 = \mu_1 \equiv \mu$ and $\nu_0 = \nu_1 \equiv \nu$. Moreover, for the purposes of this section, we fix the values of some parameters within the ranges in Table 1 as follows: $\Phi_H = 1$ host per day, $\Phi_T = 2$ ticks per day, $\varphi_1 = 1/6$ per day, and $\mu = 10^{-3}$ per day. We now derive plausible ranges for the other model parameters making use of the results from Ref. [48]. From Ref. [48, Equation (19)], we identify

$$R_{TT} = \sigma \nu_{ln} \langle k_{out} \rangle = \frac{\alpha_1 \Phi_T}{\nu_0 \nu_1}.$$

From Ref. [48] $\langle k_{out} \rangle = \frac{\Phi_T}{\nu}$, with $\langle k_{out} \rangle = 2 \times 10^2$, from which we obtain $\nu = 10^{-2}$ per day, given the fixed value of Φ_T . Ref. [48] also provides the following values: $\sigma = 0.1$ and $\nu_{ln} = 2.4 \times 10^{-3}$ or $\nu_{ln} = 2 \times 10^{-2}$ depending on the disease [48, Table 2]. Thus, we derive $\alpha_1 = \sigma \nu_{ln} \nu$, so that we conclude $\alpha_1 = 2.4 \times 10^{-6}$ or $\alpha_1 = 2 \times 10^{-5}$ per day per tick, respectively. From here, we assume values of α_1 in the interval $[10^{-6}, 10^{-4}]$.

We now turn to the transmission parameters (tick-to-host) β_1 and (host-to-tick) γ_1 . From Ref. [48, Equations (6) and (7)], we have

$$R_{TH} = \sigma \nu_{hn} = \frac{\beta_1 \Phi_H}{\mu_0 \nu_1}, \quad R_{HT} = \nu_{lh} \langle k_{out} \rangle = \frac{\gamma_1 \Phi_T}{\nu_0 (\mu_1 + \varphi_1)}.$$

Thus, we can write $\beta_1 = \sigma \mu \nu \nu_{hn} \sim 10^{-6}$, from which we define a plausible range for β_1 as $[10^{-7}, 10^{-5}]$. Finally, $\gamma_1 = \nu_{lh} (\mu + \varphi_1)$. As the value of ν_{lh} depends on the disease (it is either $\nu_{lh} = 1.9 \times 10^{-3}$ or $\nu_{lh} = 7.3 \times 10^{-2}$), we consider the interval $[10^{-5}, 10^{-2}]$ for γ_1 .

Appendix B. Within-host invasion model

Following the same steps as those provided in Section 3.2, the next-generation matrix for the within-host invasion model is given by

$$\mathbb{K} \equiv \begin{pmatrix} b_{11} & b_{12} \\ b_{21} & b_{22} \end{pmatrix},$$

where

$$\begin{aligned}
b_{11} &= \frac{\alpha_2 \bar{m}_0}{\alpha_1 \phi_{1|2} \bar{m}_1 + \nu_2} + \frac{\alpha_1 \phi_{1|2} \bar{m}_1}{\alpha_1 \phi_{1|2} \bar{m}_1 + \nu_2} \frac{\delta_2 (1 - \epsilon_c) \bar{m}_0}{\nu_c}, \\
b_{12} &= \frac{\delta_2 (1 - \epsilon_c) \bar{m}_0}{\nu_c}, \\
b_{21} &= \frac{\alpha_2 \phi_{2|1} \bar{m}_1}{\alpha_1 \phi_{1|2} \bar{m}_1 + \nu_2} + \frac{\alpha_1 \phi_{1|2} \bar{m}_1}{\alpha_1 \phi_{1|2} \bar{m}_1 + \nu_2} \frac{(\delta_1 + \delta_2) \epsilon_c (\bar{m}_0 + \phi_{2|1} \bar{m}_1) + \delta_2 (1 - \epsilon_c) \phi_{2|1} \bar{m}_1}{\nu_c}, \\
b_{22} &= \frac{(\delta_1 + \delta_2) \epsilon_c (\bar{m}_0 + \phi_{2|1} \bar{m}_1) + \delta_2 (1 - \epsilon_c) \phi_{2|1} \bar{m}_1}{\nu_c}.
\end{aligned}$$

When considering neutrality (*i.e.*, the invasive strain is the same as the resident strain), all infected tick populations (m_1 , m_2 , and m_c) are infected with the same viral strain. Thus, we have $\nu_2 = \nu_c = \nu_1$ and $\alpha_2 = \alpha_1$. We also set $\delta_1 = \delta_2 = \frac{\alpha_1}{2}$, representing that ticks in the m_c compartment will transmit virus at the same overall rate as ticks in the m_1 compartment (*i.e.*, $\delta_1 + \delta_2 = \alpha_1$). Furthermore, we would expect $\phi_{1|2} = \phi_{2|1} = 0$, since in the within-host environment (a tick) the transmitted strain is likely to be rare compared to the established strain and if the resident strain is the same as the invasive strain, then both strains have the same within-host fitness, implying that the rare transmitted strain will have no within-host advantage over the established strain, and will be unable to establish co-infection in the host (tick). With these limits, the elements of the next-generation matrix become

$$\begin{aligned}
b_{11} &= \frac{\alpha_1 \bar{m}_0}{\nu_1}, \\
b_{12} &= \frac{\alpha_1 (1 - \epsilon_c) \bar{m}_0}{2\nu_1}, \\
b_{21} &= 0, \\
b_{22} &= \frac{\alpha_1 \epsilon_c \bar{m}_0}{\nu_1}.
\end{aligned}$$

The eigenvalues are then b_{11} and b_{22} , which are equal to 1 and ϵ_c , respectively, since $\bar{m}_0 = \frac{\nu_1}{\alpha_1}$. Thus, we can conclude that $R_I = 1$, given $\epsilon_c \in [0, 1]$.

Appendix C. Alizon's proposal

Alizon [37] proposed a model with doubly infected hosts (with the same viral strain), and which seemed a sufficient approach to achieve neutral-

ity. We have considered a generalisation of the model originally proposed in Ref. [37], and which is described by the ODE system (13). By setting $\frac{dm_0}{dt} = \frac{dm_1}{dt} = \frac{dM_1}{dt} = 0$, and $m_2 = m_c = M_2 = 0$, one obtains the endemic equilibrium for the resident strain $\tilde{E}_1 = (\tilde{m}_0, \tilde{m}_1, 0, 0, \tilde{M}_1, 0)$. We then compute the invasion reproduction number of the invasive strain by considering the invasive sub-system, linearised around the resident strain endemic equilibrium, \tilde{E}_1 :

$$\begin{aligned}\frac{dm_2}{dt} &= -\nu_2 m_2 + \tilde{m}_0 \lambda_2 - m_2 (\alpha_1 \tilde{m}_1 + 2 \kappa_1 \tilde{M}_1), \\ \frac{dm_c}{dt} &= -\nu_c m_c + \tilde{m}_0 (\lambda_{1,c} + \lambda_{2,c}) + \tilde{m}_1 (\lambda_2 + \lambda_{2,c} + \Lambda_2) + m_2 (\alpha_1 \tilde{m}_1 + 2 \kappa_1 \tilde{M}_1), \\ \frac{dM_2}{dt} &= -\nu_2 M_2 + \tilde{m}_0 \Lambda_2.\end{aligned}$$

The Jacobian matrix of the invasive sub-system is

$$\tilde{J} \equiv \begin{pmatrix} -\nu_2 + \tilde{m}_0 \alpha_2 & \tilde{m}_0 \delta_2 (1 - \epsilon_c) & 2 \tilde{m}_0 \kappa_2 (1 - \epsilon_2) \\ -(\alpha_1 \tilde{m}_1 + 2 \kappa_1 \tilde{M}_1) & -\nu_c + \tilde{m}_0 (\delta_1 + \delta_2) \epsilon_c & 2 \tilde{m}_1 \kappa_2 \\ \tilde{m}_1 \alpha_2 & +\tilde{m}_1 \delta_2 & \\ +\alpha_1 \tilde{m}_1 + 2 \kappa_1 \tilde{M}_1 & & \\ 0 & 0 & -\nu_2 + 2 \tilde{m}_0 \kappa_2 \epsilon_2 \end{pmatrix},$$

and can be decomposed as follows

$$\tilde{T} \equiv \begin{pmatrix} \tilde{m}_0 \alpha_2 & \tilde{m}_0 \delta_2 (1 - \epsilon_c) & 2 \tilde{m}_0 \kappa_2 (1 - \epsilon_2) \\ \tilde{m}_1 \alpha_2 & \tilde{m}_0 (\delta_1 + \delta_2) \epsilon_c + \tilde{m}_1 \delta_2 & 2 \tilde{m}_1 \kappa_2 \\ 0 & 0 & 2 \tilde{m}_0 \kappa_2 \epsilon_2 \end{pmatrix}, \quad \text{and}$$

$$\tilde{V} \equiv \begin{pmatrix} -\nu_2 - (\alpha_1 \tilde{m}_1 + 2 \kappa_1 \tilde{M}_1) & 0 & 0 \\ \alpha_1 \tilde{m}_1 + 2 \kappa_1 \tilde{M}_1 & -\nu_c & 0 \\ 0 & 0 & -\nu_2 \end{pmatrix}.$$

Finally, the next-generation matrix, $\mathbb{K} \equiv \tilde{T}[-\tilde{V}]^{-1}$, is given by

$$\mathbb{K} \equiv \begin{pmatrix} A & B & C \\ D & E & F \\ G & H & I \end{pmatrix},$$

where

$$\begin{aligned}
A &= \frac{\alpha_2 \tilde{m}_0}{\nu_2 + \alpha_1 \tilde{m}_1 + 2\kappa_1 \tilde{M}_1} + \frac{\alpha_1 \tilde{m}_1 + 2\kappa_1 \tilde{M}_1}{\nu_2 + \alpha_1 \tilde{m}_1 + 2\kappa_1 \tilde{M}_1} \frac{\delta_2 (1 - \epsilon_c) \tilde{m}_0}{\nu_c}, \\
B &= \frac{\delta_2 (1 - \epsilon_c) \tilde{m}_0}{\nu_c}, \\
C &= \frac{2\kappa_2 (1 - \epsilon_2) \tilde{m}_0}{\nu_2}, \\
D &= \frac{\alpha_2 \tilde{m}_1}{\nu_2 + \alpha_1 \tilde{m}_1 + 2\kappa_1 \tilde{M}_1} + \frac{\alpha_1 \tilde{m}_1 + 2\kappa_1 \tilde{M}_1}{\nu_2 + \alpha_1 \tilde{m}_1 + 2\kappa_1 \tilde{M}_1} \frac{(\delta_1 + \delta_2) \epsilon_c \tilde{m}_0 + \delta_2 \tilde{m}_1}{\nu_c}, \\
E &= \frac{(\delta_1 + \delta_2) \epsilon_c \tilde{m}_0 + \delta_2 \tilde{m}_1}{\nu_c}, \\
F &= \frac{2\kappa_2 \tilde{m}_1}{\nu_2}, \\
G &= 0, \\
H &= 0, \\
I &= \frac{2\kappa_2 \epsilon_2 \tilde{m}_0}{\nu_2}.
\end{aligned}$$

The invasion reproduction number, R_I , is given by the largest eigenvalue of \mathbb{K} . One eigenvalue is given by the matrix element I . The other eigenvalues are those of the sub-matrix

$$\mathbb{K}_{2 \times 2} \equiv \begin{pmatrix} A & B \\ D & E \end{pmatrix},$$

with the largest of the two given by

$$R_I = \frac{(A + E) + \sqrt{(A + E)^2 - 4(AE - BD)}}{2}.$$

Appendix C.1. Proof of neutrality

When considering neutrality (*i.e.*, the invasive strain is the same as the resident strain), we set $\nu_2 = \nu_1 = \nu$, $v_2 = v_1 = v$, $\alpha_2 = \alpha_1 = \alpha$, $\delta_2 = \kappa_2 = \delta_1 = \kappa_1 = \kappa$, and $\epsilon_c = \epsilon_2 = \epsilon_1 = \epsilon$. Here we will show that under these neutrality conditions, $R_I = 1$, for the particular case where $\nu_0 = v = \nu$ and $\kappa = \alpha/2$. We make the simplifying assumption that infection does not affect the death rates since infection with CCHFV is asymptomatic in its animal

hosts. The assumption that $\kappa = \alpha/2$ is realistic because we are considering viral infection. As Alizon mentioned in Ref. [37], if a host infected by a given strain is re-infected by the exact same strain, we do not expect to see a change in viral load (and hence in transmission rate); that is, a singly infected tick can become doubly infected with the same strain in this model, but becoming doubly infected does not affect its viral load. Under these conditions, the endemic equilibrium for the resident strain satisfies

$$\tilde{m}_0 + \tilde{m}_1 + \widetilde{M}_1 = \frac{\Phi}{\nu}, \quad (\text{C.1})$$

with

$$\tilde{m}_0 = \frac{\nu}{\alpha}, \quad (\text{C.2})$$

$$\tilde{m}_1 = \frac{\tilde{m}_0(1 - \epsilon)(\alpha\Phi - \nu^2)}{\alpha\Phi - \nu^2\epsilon}. \quad (\text{C.3})$$

Hence, we have

$$\nu + \alpha(\tilde{m}_1 + \widetilde{M}_1) = \frac{\alpha\Phi}{\nu}. \quad (\text{C.4})$$

Making use of Eqs. (C.1), (C.2), and (C.4), the relevant elements of the next-generation matrix simplify to

$$\begin{aligned} A &= \frac{\alpha\tilde{m}_0}{\nu + \alpha(\tilde{m}_1 + \widetilde{M}_1)} + \frac{\alpha(\tilde{m}_1 + \widetilde{M}_1)}{\nu + \alpha(\tilde{m}_1 + \widetilde{M}_1)} \frac{\alpha(1 - \epsilon)\tilde{m}_0}{2\nu}, \\ &= \frac{1}{\Phi} \left[\nu\tilde{m}_0 + \frac{1}{2}\nu(1 - \epsilon) \left(\frac{\Phi}{\nu} - \tilde{m}_0 \right) \right], \\ B &= \frac{\alpha(1 - \epsilon)\tilde{m}_0}{2\nu} = \frac{1}{2}(1 - \epsilon), \\ D &= \frac{\alpha\tilde{m}_1}{\nu + \alpha(\tilde{m}_1 + \widetilde{M}_1)} + \frac{\alpha(\tilde{m}_1 + \widetilde{M}_1)}{\nu + \alpha(\tilde{m}_1 + \widetilde{M}_1)} \frac{\alpha\epsilon\tilde{m}_0 + \frac{1}{2}\alpha\tilde{m}_1}{\nu}, \\ &= \frac{1}{\Phi} \left[\nu\tilde{m}_1 + \nu \left(\epsilon + \frac{\alpha}{2\nu}\tilde{m}_1 \right) \left(\frac{\Phi}{\nu} - \tilde{m}_0 \right) \right], \\ E &= \frac{\alpha\epsilon\tilde{m}_0 + \frac{1}{2}\alpha\tilde{m}_1}{\nu} = \epsilon + \frac{\alpha}{2\nu}\tilde{m}_1, \\ I &= \frac{\alpha\epsilon\tilde{m}_0}{\nu} = \epsilon. \end{aligned}$$

Since $I = \epsilon \leq 1$, we need to show that

$$R_I = \frac{(A + E) + \sqrt{(A + E)^2 - 4(AE - BD)}}{2} = 1.$$

It can be shown that this is true if and only if

$$A + E - (AE - BD) = 1. \quad (\text{C.5})$$

Thus, in order to show that $R_I = 1$, it is sufficient to show that Eq. (C.5) holds. We have,

$$AE - BD = \frac{1}{\Phi} \epsilon \nu \left(\tilde{m}_0 + \frac{1}{2} \tilde{m}_1 \right).$$

Thus, we can write

$$\begin{aligned} A + E - (AE - BD) &= \frac{1}{\Phi} \left[\nu \tilde{m}_0 + \frac{1}{2} \nu (1 - \epsilon) \left(\frac{\Phi}{\nu} - \tilde{m}_0 \right) + \Phi \epsilon + \frac{\alpha \Phi}{2\nu} \tilde{m}_1 - \epsilon \nu \left(\tilde{m}_0 + \frac{1}{2} \tilde{m}_1 \right) \right], \\ &= \frac{1}{\Phi} \left[\frac{1}{2} \nu \tilde{m}_0 (1 - \epsilon) + \frac{\Phi}{2} (1 + \epsilon) + \frac{1}{2\nu} \tilde{m}_1 (\alpha \Phi - \nu^2 \epsilon) \right]. \end{aligned}$$

Substituting \tilde{m}_1 with its expression from Eq. (C.3) gives

$$A + E - (AE - BD) = \frac{1}{\Phi} \left[\frac{\alpha \Phi}{2\nu} \tilde{m}_0 (1 - \epsilon) + \frac{\Phi}{2} (1 + \epsilon) \right].$$

Finally, by substituting Eq. (C.2) in the previous equation, we have

$$A + E - (AE - BD) = 1.$$

Appendix D. The two-slot model of co-infection and co-transmission

Appendix D.1. Transmission events

We list here the transmission events which lead to the two-slot mathematical model introduced in Eq. (15) grouped by the type of transmission. T_0 denotes a susceptible tick, T_1 and T_2 denote a singly infected tick with V_1 and V_2 , respectively, T_{11} and T_{22} denote a doubly infected tick with V_1 and V_2 , respectively, and T_c denotes a co-infected tick (with V_1 and V_2).

- Transmission from a singly infected tick to a susceptible tick:

$$T_0 + T_1 \rightarrow T_1 + T_1 \text{ with rate } \alpha_1 m_0 m_1,$$

$$T_0 + T_2 \rightarrow T_2 + T_2 \text{ with rate } \alpha_2 m_0 m_2.$$

- Transmission from a singly infected tick to a singly infected tick:

$$T_1 + T_1 \rightarrow T_{11} + T_1 \text{ with rate } \alpha_1 m_1 m_1,$$

$$T_1 + T_2 \rightarrow T_c + T_2 \text{ with rate } \alpha_2 m_1 m_2,$$

$$T_2 + T_1 \rightarrow T_c + T_1 \text{ with rate } \alpha_1 m_2 m_1,$$

$$T_2 + T_2 \rightarrow T_{22} + T_2 \text{ with rate } \alpha_2 m_2 m_2.$$

- Transmission from a doubly infected tick to a susceptible tick:

$$T_0 + T_{11} \rightarrow T_1 + T_{11} \text{ with rate } (1 - \epsilon_1) 2\kappa_1 m_0 M_1,$$

$$T_0 + T_{11} \rightarrow T_{11} + T_{11} \text{ with rate } \epsilon_1 2\kappa_1 m_0 M_1.$$

$$T_0 + T_{22} \rightarrow T_2 + T_{22} \text{ with rate } (1 - \epsilon_2) 2\kappa_2 m_0 M_2,$$

$$T_0 + T_{22} \rightarrow T_{22} + T_{22} \text{ with rate } \epsilon_2 2\kappa_2 m_0 M_2.$$

- Transmission from a co-infected tick to a susceptible tick:

$$T_0 + T_c \rightarrow T_1 + T_c \text{ with rate } (1 - \epsilon_c) \delta_1 m_0 m_c,$$

$$T_0 + T_c \rightarrow T_2 + T_c \text{ with rate } (1 - \epsilon_c) \delta_2 m_0 m_c,$$

$$T_0 + T_c \rightarrow T_c + T_c \text{ with rate } \frac{2\delta_1 \delta_2}{\delta_1 + \delta_2} \epsilon_c m_0 m_c,$$

$$T_0 + T_c \rightarrow T_{11} + T_c \text{ with rate } \frac{\delta_1^2}{\delta_1 + \delta_2} \epsilon_c m_0 m_c,$$

$$T_0 + T_c \rightarrow T_{22} + T_c \text{ with rate } \frac{\delta_2^2}{\delta_1 + \delta_2} \epsilon_c m_0 m_c.$$

- Transmission from a co-infected tick to a singly infected tick:

$$T_1 + T_c \rightarrow T_{11} + T_c \text{ with rate } \delta_1 m_1 m_c,$$

$$T_1 + T_c \rightarrow T_c + T_c \text{ with rate } \delta_2 m_1 m_c.$$

$$T_2 + T_c \rightarrow T_{22} + T_c \text{ with rate } \delta_2 m_2 m_c,$$

$$T_2 + T_c \rightarrow T_c + T_c \text{ with rate } \delta_1 m_2 m_c.$$

- Transmission from a doubly infected tick to a singly infected tick:

$$T_1 + T_{11} \rightarrow T_{11} + T_{11} \text{ with rate } 2\kappa_1 m_1 M_1,$$

$$T_2 + T_{22} \rightarrow T_{22} + T_{22} \text{ with rate } 2\kappa_2 m_2 M_2,$$

$$T_1 + T_{22} \rightarrow T_c + T_{22} \text{ with rate } 2\kappa_2 m_1 M_2,$$

$$T_2 + T_{11} \rightarrow T_c + T_{11} \text{ with rate } 2\kappa_1 m_2 M_1.$$

Appendix D.2. Existence of the endemic equilibrium of V_1

In Appendix C.1 we have shown the endemic equilibrium (EE) of V_1 can be written as $\tilde{E}_1 = (\tilde{m}_0, \tilde{m}_1, 0, 0, \tilde{M}_1, 0)$. We have also shown the neutrality of the invasion reproduction number in Alizon's model under the assumption $\kappa = \alpha/2$. This assumption simplifies the next-generation matrix and helps to prove neutrality. Our two-slot model, as an extension of Alizon's model, shares the same resident strain EE. In this section, we will discuss the existence of the resident strain EE when $\kappa \neq \alpha/2$, referring to Appendix C.1 for the case $\kappa = \alpha/2$. We, thus, write the EE as $E'_1 = (m'_0, m'_1, 0, 0, M'_1, 0)$. We then compute the invasion reproduction number R'_I and prove the neutrality in Appendix D.3 and Appendix D.4, respectively.

First, we consider the resident sub-system, where $m_2 = m_C = M_2 = 0$ and assume $\nu_0 = \nu_1 = \nu_2 = \nu_c = \nu_1 = \nu_2 = \nu$, without loss of generality. We have

$$\begin{aligned}\frac{dm_0}{dt} &= \Phi - \nu m_0 - (\alpha_1 m_1 + 2 \kappa_1 M_1) m_0, \\ \frac{dm_1}{dt} &= -\nu m_1 - (\alpha_1 m_1 + 2 \kappa_1 M_1) m_1 + (\alpha_1 m_1 + 2 \kappa_1 (1 - \epsilon_1) M_1) m_0, \\ \frac{dM_1}{dt} &= -\nu M_1 + (\alpha_1 m_1 + 2 \kappa_1 M_1) m_1 + 2 \epsilon_1 \kappa_1 M_1 m_0.\end{aligned}\tag{D.1}$$

We compute the basic reproduction number of this sub-system at the VFE $E_0 = (m_0^*, 0, 0, 0, 0, 0)$, where $m_0^* = \frac{\Phi}{\nu}$. We can write

$$R'_1 = \max \left\{ \frac{\Phi \alpha_1}{\nu^2}, \frac{2 \Phi \epsilon_1 \kappa_1}{\nu^2} \right\}.\tag{D.2}$$

By setting $\frac{d(m_1+M_1)}{dt} = 0$ and $\frac{dm_0}{dt} = 0$, we obtain the following equations:

$$\alpha_1 m'_1 + 2 \kappa_1 M'_1 = \frac{(m'_1 + M'_1) \nu}{m'_0},\tag{D.3}$$

$$m'_1 + M'_1 = \frac{\Phi}{\nu} - m'_0.\tag{D.4}$$

From Eq. (D.4), we have $m'_0 < \frac{\Phi}{\nu}$ to ensure positive m'_1 and M'_1 . By combining Eqs. (D.3) and (D.4), we then get

$$\alpha_1 m'_1 + 2 \kappa_1 M'_1 = \frac{\Phi}{m'_0} - \nu.\tag{D.5}$$

By solving Eq. (D.4) and Eq. (D.5), one obtains

$$m'_1 = \frac{\Phi - \nu m'_0}{2\kappa_1 - \alpha_1} \left(\frac{1}{m'_0} - \frac{\alpha_1}{\nu} \right), \quad \text{and} \quad M'_1 = \frac{\Phi - \nu m'_0}{\alpha_1 - 2\kappa_1} \left(\frac{1}{m'_0} - \frac{2\kappa_1}{\nu} \right). \quad (\text{D.6})$$

We conclude that to ensure positive values for m'_1 and M'_1 , we require the following conditions:

- if $\alpha_1 > 2\kappa_1$, $\frac{\nu}{\alpha_1} < m'_0 < \frac{\nu}{2\kappa_1}$, or
- if $\alpha_1 < 2\kappa_1$, $\frac{\nu}{2\kappa_1} < m'_0 < \frac{\nu}{\alpha_1}$.

If $2\kappa_1 = \alpha_1$, we refer to Appendix C.1. Substituting Eqs. (D.5) and (D.6) into $\frac{dM_1}{dt} = 0$, we derive the following cubic equation for m'_0 :

$$Q(m_0) = A_3 m_0^3 + A_2 m_0^2 + A_1 m_0 + A_0 = 0,$$

where $A_3 = -2\kappa_1 \epsilon_1 \alpha_1$, $A_2 = 2\kappa_1 \epsilon_1 \nu - 2\kappa_1 \nu + \alpha_1 \nu$, $A_1 = 2\Phi \kappa_1$, and $A_0 = -\Phi \nu$. It is easy to observe that $A_3 < 0$, $Q(0) < 0$, and $Q'(0) > 0$. We therefore have one negative root for $Q(m'_0) = 0$ and two critical points (*i.e.*, where $Q'(m'_0) = 0$) distributed at different sides of the y -axis. From Eqs. (D.4) and (D.6), we have three important values for m'_0 : $\frac{\Phi}{\nu}$, $\frac{\nu}{\alpha_1}$, and $\frac{\nu}{2\kappa_1}$. We then have the following values:

$$\begin{aligned} Q\left(\frac{\Phi}{\nu}\right) &= \Phi \nu \left(1 - \frac{\Phi 2\kappa_1 \epsilon_1}{\nu} \right) \left(\frac{\Phi \alpha_1}{\nu} - 1 \right), \\ Q\left(\frac{\nu}{\alpha_1}\right) &= \nu^2 \left(\frac{\Phi}{\nu} - \frac{\nu}{\alpha_1} \right) \left(\frac{2\kappa_1}{\alpha_1} - 1 \right), \\ Q\left(\frac{\nu}{2\kappa_1}\right) &= \frac{\nu^3}{2\kappa_1} \left(\frac{\alpha_1}{2\kappa_1} - 1 \right) (1 - \epsilon_1). \end{aligned}$$

We can now discuss the existence of a real and positive m'_0 , when $R'_1 > 1$ and $0 \leq \epsilon_1 \leq 1$. We need to consider the following cases:

- (i) when $\frac{2\kappa_1 \epsilon_1 \Phi}{\nu^2} \leq 1 < \frac{\alpha_1 \Phi}{\nu^2}$, then $R'_1 = \frac{\alpha_1 \Phi}{\nu^2}$, $Q\left(\frac{\Phi}{\nu}\right) \geq 0$ and $\frac{\nu}{\alpha_1} < \frac{\Phi}{\nu}$, $\frac{\nu}{2\kappa_1} \geq \epsilon_1 \frac{\Phi}{\nu}$. We need to consider two separate cases:
 - (a) if $\alpha_1 > 2\kappa_1$, that is, $\frac{\nu}{\alpha_1} < m'_0 < \frac{\nu}{2\kappa_1}$, then $Q\left(\frac{\nu}{\alpha_1}\right) < 0$, and $Q\left(\frac{\nu}{2\kappa_1}\right) \geq 0$. We thus have a unique solution for $Q(m'_0) = 0$ on $\left(\frac{\nu}{\alpha_1}, \min\left\{\frac{\nu}{2\kappa_1}, \frac{\Phi}{\nu}\right\}\right]$.

- (b) if $\alpha_1 < 2\kappa_1$, that is, $\frac{\nu}{2\kappa_1} < m'_0 < \frac{\nu}{\alpha_1}$ and $2\kappa_1\epsilon_1 < \alpha_1 < 2\kappa_1$, then $Q\left(\frac{\nu}{\alpha_1}\right) > 0$ and $Q\left(\frac{\nu}{2\kappa_1}\right) \leq 0$. We thus have a unique solution on $\left[\frac{\nu}{2\kappa_1}, \frac{\nu}{\alpha_1}\right)$.
- (ii) when $\frac{\alpha_1\Phi}{\nu^2} \leq 1 < \frac{2\kappa_1\epsilon_1\Phi}{\nu^2}$, then $R'_1 = \frac{2\kappa_1\epsilon_1\Phi}{\nu^2}$, $\alpha_1 < 2\kappa_1\epsilon_1 < 2\kappa_1$, $\frac{\nu}{2\kappa_1} < \epsilon_1\frac{\Phi}{\nu}$, and $\frac{\nu}{\alpha_1} \geq \frac{\Phi}{\nu}$, since $\alpha_1 < 2\kappa_1$; that is, $\frac{\nu}{2\kappa_1} < m'_0 < \frac{\nu}{\alpha_1}$. Then we can further constrain the solution to $\frac{\nu}{2\kappa_1} < m'_0 < \frac{\Phi}{\nu}$, and we have $Q\left(\frac{\nu}{2\kappa_1}\right) \leq 0$, and $Q\left(\frac{\Phi}{\nu}\right) > 0$. Thus a unique solution can be found on $\left[\frac{\nu}{2\kappa_1}, \frac{\Phi}{\nu}\right)$.
- (iii) when $\frac{\alpha_1\Phi}{\nu^2} > 1$ and $\frac{2\kappa_1\epsilon_1\Phi}{\nu^2} > 1$, then $\frac{\nu}{\alpha_1} < \frac{\Phi}{\nu}$, $\frac{\nu}{2\kappa_1} < \epsilon_1\frac{\Phi}{\nu}$, and $Q\left(\frac{\Phi}{\nu}\right) < 0$. We need to consider two different cases:
- (a) if $\alpha_1 > 2\kappa_1$, that is $\frac{\nu}{\alpha_1} < m'_0 < \frac{\nu}{2\kappa_1}$, then $Q\left(\frac{\nu}{\alpha_1}\right) < 0$ and $Q\left(\frac{\nu}{2\kappa_1}\right) \geq 0$. We thus have a unique solution on $\left(\frac{\nu}{\alpha_1}, \frac{\nu}{2\kappa_1}\right]$.
- (b) if $\alpha_1 < 2\kappa_1$, that is $\frac{\nu}{2\kappa_1} < m'_0 < \frac{\nu}{\alpha_1}$, then $Q\left(\frac{\nu}{\alpha_1}\right) > 0$ and $Q\left(\frac{\nu}{2\kappa_1}\right) \leq 0$. We thus have a unique solution on $\left[\frac{\nu}{2\kappa_1}, \frac{\nu}{\alpha_1}\right)$.

Therefore, when $R'_1 > 1$ and $0 \leq \epsilon_1 \leq 1$, a unique real and non-negative solution of $E'_1 = (m'_0, m'_1, 0, 0, M'_1, 0)$ is guaranteed. We can ensure three real roots (*i.e.*, one negative and two positive roots) for $Q(m_0) = 0$, such that we identify the value of m'_0 which is real and positive, with m'_1 and M'_1 real and positive as well. To do so we make use of the general formula for a cubic equation (with $A_3 \neq 0$) [56]:

$$m'_0 = -\frac{1}{3A_3} \left(A_2 + \Delta + \frac{\Delta_0}{\Delta} \right), \quad (\text{D.7})$$

with

$$\begin{aligned} \Delta_0 &= A_2^2 - 3A_1A_3, \\ \Delta_1 &= 2A_2^3 - 9A_1A_2A_3 + 27A_0A_3^2, \\ \Delta &= \left(\frac{-1 + \sqrt{-3}}{2} \right)^2 \left(\frac{\Delta_1 + \sqrt{\Delta_1^2 - 4\Delta_0^3}}{2} \right)^{1/3}. \end{aligned}$$

We note that m'_0 is real even though Δ is a complex number. Another expression for the solution of m'_0 making use of trigonometric functions can be found in Ref. [57].

Appendix D.3. Invasion reproduction number

We can now compute the invasion reproduction number, R'_I , of V_2 for the invasion sub-system, linearised around the endemic equilibrium E'_1 . We have the following Jacobian matrix:

$$J' \equiv \begin{pmatrix} -\nu - \alpha_1 m'_1 & \delta_2 (1 - \epsilon_c) m'_0 & 2 \kappa_2 (1 - \epsilon_2) m'_0 \\ +\alpha_2 m'_0 - 2 \kappa_1 M'_1 & -\nu + \delta_2 \left(\frac{2\delta_1 \epsilon_c}{\delta_1 + \delta_2} m'_0 + m'_1 \right) & 2 \kappa_2 m'_1 \\ \frac{(\alpha_1 + \alpha_2) m'_1}{+2 \kappa_1 M'_1} & \frac{\delta_2^2 \epsilon_c}{\delta_1 + \delta_2} m'_0 & -\nu + 2 \epsilon_2 \kappa_2 m'_0 \\ 0 & & \end{pmatrix},$$

which can be decomposed as follows

$$T' \equiv \begin{pmatrix} \alpha_2 m'_0 & \delta_2 (1 - \epsilon_c) m'_0 & 2 \kappa_2 (1 - \epsilon_2) m'_0 \\ \alpha_2 m'_1 & \delta_2 \left(\frac{2\delta_1 \epsilon_c}{\delta_1 + \delta_2} m'_0 + m'_1 \right) & 2 \kappa_2 m'_1 \\ 0 & \frac{\delta_2^2 \epsilon_c}{\delta_1 + \delta_2} m'_0 & 2 \epsilon_2 \kappa_2 m'_0 \end{pmatrix},$$

and

$$V' \equiv \begin{pmatrix} -\nu - \alpha_1 m'_1 - 2 \kappa_1 M'_1 & 0 & 0 \\ \alpha_1 m'_1 + 2 \kappa_1 M'_1 & -\nu & 0 \\ 0 & 0 & -\nu \end{pmatrix}.$$

We can compute the next-generation matrix, $\mathbb{K}' = T'[-V']^{-1}$, given by:

$$\mathbb{K}' \equiv \begin{pmatrix} d_{11} & d_{12} & d_{13} \\ d_{21} & d_{22} & d_{23} \\ d_{31} & d_{32} & d_{33} \end{pmatrix},$$

where

$$\begin{aligned}
d_{11} &= \frac{\alpha_2 m'_0 + \delta_2 (1 - \epsilon_c) (m'_1 + M'_1)}{\Phi} m'_0, \\
d_{12} &= \frac{\delta_2}{\nu} (1 - \epsilon_c) m'_0, \\
d_{13} &= \frac{2 \kappa_2}{\nu} (1 - \epsilon_2) m'_0, \\
d_{21} &= \frac{\alpha_2}{\Phi} m'_0 m'_1 + \frac{\delta_2}{\Phi} \left(\frac{2 \delta_1 \epsilon_c}{\delta_1 + \delta_2} m'_0 + m'_1 \right) (m'_1 + M'_1), \\
d_{22} &= \frac{\delta_2}{\nu} \left(\frac{2 \epsilon_c \delta_1}{\delta_1 + \delta_2} m'_0 + m'_1 \right), \\
d_{23} &= \frac{2 \kappa_2}{\nu} m'_1, \\
d_{31} &= \frac{\delta_2}{\Phi} \frac{\epsilon_c \delta_2}{\delta_1 + \delta_2} m'_0 (m'_1 + M'_1), \\
d_{32} &= \frac{\delta_2}{\nu} \frac{\epsilon_c \delta_2}{\delta_1 + \delta_2} m'_0, \\
d_{33} &= \frac{2 \epsilon_2 \kappa_2}{\nu} m'_0.
\end{aligned}$$

We can obtain the invasion reproduction number, R'_I , as a function of m'_0 by substituting Eq. (D.6) into \mathbb{K}' and computing its largest eigenvalue.

Appendix D.4. Proof of neutrality

We consider the following limits: $\alpha_1, \alpha_2 \rightarrow \alpha$, $\kappa_1, \kappa_2, \delta_1, \delta_2 \rightarrow \kappa$, and $\epsilon_1, \epsilon_2, \epsilon_c \rightarrow \epsilon$. In this limit, we can write the invasion reproduction number,

R'_I , at neutrality as follows:

$$\begin{aligned}
R'_I = \frac{m'_0}{2\nu\Phi(\Phi - \alpha\epsilon m'^2_0)} \left\{ \right. \\
& 2\Phi^2\kappa + \Phi\nu(\alpha - 2\kappa(1 - \epsilon))m'_0 \\
& - \Phi\alpha\epsilon\kappa(1 + \epsilon)m'^2_0 - \alpha\epsilon\nu(\alpha - \kappa(1 - \epsilon))m'^3_0 \\
& + \left[4\Phi\alpha\epsilon\kappa\nu m'_0 (\Phi - \alpha\epsilon m'^2_0) (\Phi(-3 + \epsilon) + m'_0(\nu(1 - \epsilon) + 2\alpha\epsilon m'_0)) \right. \\
& \quad + \left(2\Phi^2\kappa + m'_0(\Phi\nu(\alpha - 2\kappa(1 - \epsilon)) \right. \\
& \quad \left. \left. - \epsilon\alpha m'_0((1 + \epsilon)\Phi\kappa + \nu m'_0(\alpha - (1 - \epsilon)\kappa)) \right) \right]^{1/2} \left. \right\}. \tag{D.8}
\end{aligned}$$

Now we can prove the neutrality of R'_I in two scenarios:

(1) when $\kappa = \alpha/2$, the expression for R'_I reduces to

$$\begin{aligned}
R'_I = \frac{\alpha m'_0 (2\Phi(\Phi + \epsilon\nu m'_0) - \epsilon\alpha(1 + \epsilon)(\Phi + \nu m'_0)m'^2_0)}{4\Phi\nu(\Phi - \epsilon\alpha m'^2_0)} \\
+ \alpha m'_0 \left[\frac{\epsilon m'_0 ((2\epsilon\alpha m'_0 + (1 - \epsilon)\nu)m'_0 - (3 - \epsilon)\Phi)}{2\nu\Phi(\Phi - \epsilon\alpha m'^2_0)} \right. \\
\left. + \left(\frac{2\Phi^2 + \epsilon m'_0 (2\Phi\nu - \alpha m'_0(1 + \epsilon)(\Phi + \nu m'_0))}{4\Phi\nu(\Phi - \epsilon\alpha m'^2_0)} \right)^2 \right]^{1/2}.
\end{aligned}$$

By substituting $m'_0 = \tilde{m}_0 = \nu/\alpha$ as in Eq. (C.2), we obtain $R'_I \equiv 1$, as desired.

(2) when $\kappa \neq \alpha/2$, the expression for R'_I cannot be easily simplified. In this case, we perform a numerical study, making use of Mathematica to prove neutrality, which requires the expression of m'_0 from Eq. (D.7).

Acknowledgements

We thank Dr. Jonathan Carruthers (UKHSA) for preparing Figure 1, and Dr. Macauley Locke (LANL) for research discussions on model development and parameterisation.

Funding

This work was supported by the Biotechnology and Biological Sciences Research Council Research Council [grant number BB/W010755/1] (B.W., Z.V., M.L.-G., and G.L.). This study was supported by the National Institutes of Health/National Institute of Allergy and Infectious Diseases grant R01AI087520 to T.L., and grant R01AI167048 to E.R.-S., T.L. and C.M.-P. This project has received funding from the European Union’s Horizon 2020 research and innovation program under the Marie Skłodowska-Curie Grant, agreement number 764698 (G.B., G.L. and C.M.-P.). Y.L.’s research was partially supported by the NSF of China [12071393].

Data availability statement

Numerical codes (Python) to reproduce Figure 2 and Figure 4, as well as the Mathematica notebook to reproduce proofs and results from Appendix D, are deposited at https://github.com/MolEvolEpid/coinfection_cotransmission_cofeeding_in_ticks.

Selected references

1. Maliyoni *et al.* [15] proposed a stochastic model for the dynamics of two tick-transmitted pathogens in a single tick population. The model, a continuous-time Markov chain based on a deterministic tick-borne disease model, was used to investigate the duration of possible pathogen co-existence and the probability of pathogen extinction.
2. Cutler *et al.* [16] reviewed current understanding of co-infection in tick-borne diseases affecting both tick and vertebrate host populations, highlighting the need for more research on pathogen interactions.
3. Vogels *et al.* [20] reviewed the impact of co-infection on clinical disease in humans, discussed the possibility for co-transmission from mosquito to human, and described a role for modeling transmission dynamics at various levels of co-transmission with the aim of understanding whether virus co-infections should be viewed as a serious concern for public health.
4. Meehan *et al.* [22] investigated the stochastic dynamics of the emergence of a novel disease strain, which is introduced into a population in which it competes with a resident endemic strain. The analysis is

carried out by means of a branching process approximation to calculate the probability that the new strain becomes established.

5. Allen *et al.* [24] formulated a general epidemiological model for one vector species and one plant species with potential co-infection in the host plant by two viruses. First, the basic reproduction number is derived, and thus, conditions for successful invasion of a single virus are determined. Then, a new invasion threshold is derived to provide conditions for successful invasion of a second virus.
6. White *et al.* [25] proposed a mathematical model for a two-pathogen, one-tick, one-host system with the aim of determining how long an invading pathogen persists within a tick population in which a resident pathogen is already established.
7. Rovenolt *et al.* [29] developed a model of two co-infected host species to understand under which conditions co-infection can interfere with parasite-mediated apparent competition among hosts.
8. Le *et al.* [30] studied a Susceptible-Infected-Susceptible (SIS) compartmental model with two strains and co-infection/co-colonization, incorporating five strain fitness dimensions under the same framework to understand coexistence and competition mechanisms.
9. Alizon [36] discussed how multiple infections have been modelled in evolutionary epidemiology, presenting within-host models, super-infection frameworks, co-infection models, and some perspectives for the study of multiple infections in evolutionary epidemiology. In particular, he showed that a widely used co-infection model is *not neutral* as it confers a frequency-dependent advantage to rare neutral mutants.
10. Alizon [37] studied the effect of co-transmission on virulence evolution when parasites compete for host resources.
11. Bhowmick *et al.* [38] developed a compartment-based non-linear ordinary differential equation system to model the disease transmission cycle including blood-sucking ticks, livestock and humans. Sensitivity analysis of the basic reproduction number shows that decreasing the tick survival time is an efficient method to control the disease. They concluded that in the case of CCHFV transmission due to co-feeding, as well as trans-stadial and trans-ovarial transmission, are important routes to sustain the disease cycle.
12. Hoch *et al.* [44] proposed a dynamic mechanistic model that takes into account the major processes involved in tick population dynamics and

pathogen transmission with the aim of testing potential scenarios for pathogen control.

13. Johnstone *et al.* [48] derived expressions for the basic reproduction number and the related tick type-reproduction number accounting for the observation that larval and nymphal ticks tend to aggregate on the same minority of hosts (tick co-aggregation and co-feeding). The pattern of tick blood meals is represented as a directed, acyclic, bipartite contact network.
14. Belluccini [51] proposed both deterministic and stochastic models of co-infection with tick-borne viruses to investigate the role that different routes of transmission play in the spread of infectious diseases and to study the probability and timescale of co-infection events.
15. Maliyoni *et al.* [52] investigated the impact of between-patch migration on the dynamics of a tick-borne disease on disease extinction and persistence making use of a system of stochastic differential equations.
16. Lin *et al.* [55] studied the impact of Zika and Dengue virus co-infection on viral infection, examining viral replication activity in cells infected simultaneously, or sequentially.

References

- [1] S. M. McDonald, M. I. Nelson, P. E. Turner, J. T. Patton, Reassortment in segmented RNA viruses: mechanisms and outcomes, *Nature Reviews Microbiology* 14 (7) (2016) 448–460.
- [2] M. Pérez-Losada, M. Arenas, J. C. Galán, F. Palero, F. González-Candelas, Recombination in viruses: mechanisms, methods of study, and evolutionary consequences, *Infection, Genetics and Evolution* 30 (2015) 296–307.
- [3] A. Negredo, R. Sánchez-Arroyo, F. Díez-Fuertes, F. De Ory, M. A. Budiño, A. Vázquez, Á. Garcinuño, L. Hernández, C. de la Hoz González, A. Gutiérrez-Arroyo, et al., Fatal case of Crimean-Congo hemorrhagic fever caused by reassortant virus, Spain, 2018, *Emerging Infectious Diseases* 27 (4) (2021) 1211.
- [4] S. R. Gerrard, L. Li, A. D. Barrett, S. T. Nichol, Ngari virus is a Bunyamwera virus reassortant that can be associated with large outbreaks

- of hemorrhagic fever in Africa, *Journal of virology* 78 (16) (2004) 8922–8926.
- [5] T. D. Cline, E. A. Karlsson, P. Freiden, B. J. Seufzer, J. E. Rehg, R. J. Webby, S. Schultz-Cherry, Increased pathogenicity of a reassortant 2009 pandemic H1N1 influenza virus containing an H5N1 hemagglutinin, *Journal of virology* 85 (23) (2011) 12262–12270.
- [6] <https://www.who.int/blueprint/en/>.
- [7] A. Portillo, A. M. Palomar, P. Santibáñez, J. A. Oteo, Epidemiological aspects of Crimean-Congo hemorrhagic fever in Western Europe: what about the future?, *Microorganisms* 9 (3) (2021) 649.
- [8] A. Fanelli, D. Buonavoglia, Risk of Crimean-Congo haemorrhagic fever virus introduction and spread in CCHF-free countries in Southern and Western Europe: A semi-quantitative risk assessment, *One Health* 13 (2021) 100290.
- [9] J. Mosquera, F. R. Adler, Evolution of virulence: a unified framework for co-infection and super-infection, *Journal of Theoretical Biology* 195 (3) (1998) 293–313.
- [10] L. J. Allen, N. Kirupaharan, Asymptotic dynamics of deterministic and stochastic epidemic models with multiple pathogens, *International Journal of Numerical Analysis and Modeling* 2 (3) (2005) 329–344.
- [11] X.-S. Zhang, D. De Angelis, P. J. White, A. Charlett, R. G. Pebody, J. McCauley, Co-circulation of influenza a virus strains and emergence of pandemic via reassortment: the role of cross-immunity, *Epidemics* 5 (1) (2013) 20–33.
- [12] H. C. Slater, M. Gambhir, P. E. Parham, E. Michael, Modelling co-infection with malaria and lymphatic filariasis, *PLoS Computational Biology* 9 (6) (2013) e1003096.
- [13] L. Yakob, G. M. Williams, D. J. Gray, K. Halton, J. A. Solon, A. C. Clements, Slaving and release in co-infection control, *Parasites & Vectors* 6 (2013) 1–9.

- [14] S. Lass, P. J. Hudson, J. Thakar, J. Saric, E. Harvill, R. Albert, S. E. Perkins, Generating super-shedders: co-infection increases bacterial load and egg production of a gastrointestinal helminth, *Journal of the Royal Society Interface* 10 (80) (2013) 20120588.
- [15] M. Maliyoni, F. Chirove, H. D. Gaff, K. S. Govinder, A stochastic epidemic model for the dynamics of two pathogens in a single tick population, *Theoretical Population Biology* 127 (2019) 75–90, (*).
- [16] S. J. Cutler, M. Vayssier-Taussat, A. Estrada-Peña, A. Potkonjak, A. D. Mihalca, H. Zeller, Tick-borne diseases and co-infection: Current considerations, *Ticks and tick-borne diseases* 12 (1) (2021) 101607, (*).
- [17] F. M. Pabon-Rodriguez, G. D. Brown, B. M. Scorza, C. A. Petersen, Bayesian multivariate longitudinal model for immune responses to Leishmania: A tick-borne co-infection study, *Statistics in Medicine* (2023).
- [18] D. Gao, T. C. Porco, S. Ruan, Coinfection dynamics of two diseases in a single host population, *Journal of mathematical analysis and applications* 442 (1) (2016) 171–188.
- [19] Y. Lou, L. Liu, D. Gao, Modeling co-infection of Ixodes tick-borne pathogens, *Mathematical Biosciences & Engineering* 14 (5&6) (2017) 1301.
- [20] C. B. Vogels, C. Rückert, S. M. Cavany, T. A. Perkins, G. D. Ebel, N. D. Grubaugh, Arbovirus coinfection and co-transmission: A neglected public health concern?, *PLoS biology* 17 (1) (2019) e3000130, (*).
- [21] P. C. Cross, J. O. Lloyd-Smith, P. L. F. Johnson, W. M. Getz, Duelling timescales of host movement and disease recovery determine invasion of disease in structured populations, *Ecology Letters* 183 (2005) 587–595. doi:10.1111/j.1461-0248.2005.00760.x.
- [22] M. T. Meehan, R. C. Cope, E. S. McBryde, On the probability of strain invasion in endemic settings: accounting for individual heterogeneity and control in multi-strain dynamics, *Journal of Theoretical Biology* 487 (2020) 110109, (*).
- [23] S. Alizon, J. C. De Roode, Y. Michalakis, Multiple infections and the evolution of virulence, *Ecology Letters* 16 (4) (2013) 556–567.

- [24] L. J. Allen, V. A. Bokil, N. J. Cunniffe, F. M. Hamelin, F. M. Hilker, M. J. Jeger, Modelling vector transmission and epidemiology of co-infecting plant viruses, *Viruses* 11 (12) (2019) 1153, (*).
- [25] A. White, E. Schaefer, C. W. Thompson, C. M. Kribs, H. Gaff, Dynamics of two pathogens in a single tick population, *Letters in Biomathematics* 6 (1) (2019) 50, (*).
- [26] M. Bushman, R. Antia, A general framework for modelling the impact of co-infections on pathogen evolution, *Journal of the Royal Society Interface* 16 (155) (2019) 20190165.
- [27] W. O. Kermack, A. G. McKendrick, A contribution to the mathematical theory of epidemics, *Proceedings of the Royal Society of London, Series A* 115 (772) (1927) 700–721.
- [28] F. Pfab, R. M. Nisbet, C. J. Briggs, A time-since-infection model for populations with two pathogens, *Theoretical Population Biology* 144 (2022) 1–12.
- [29] F. H. Rovenolt, A. T. Tate, The impact of coinfection dynamics on host competition and coexistence, *The American Naturalist* 199 (1) (2022) 91–107, (*).
- [30] T. M. T. Le, S. Madec, E. Gjini, Disentangling how multiple traits drive two strain frequencies in SIS dynamics with coinfection, *Journal of Theoretical Biology* 538 (2022) 111041, (*).
- [31] C. M. Saad-Roy, B. T. Grenfell, S. A. Levin, L. Pellis, H. B. Stage, P. Van Den Driessche, N. S. Wingreen, Superinfection and the evolution of an initial asymptomatic stage, *Royal Society Open Science* 8 (1) (2021) 202212.
- [32] A. A. McLaughlin, L. Hanley-Bowdoin, G. G. Kennedy, A. L. Jacobson, Vector acquisition and co-inoculation of two plant viruses influences transmission, infection, and replication in new hosts, *Scientific Reports* 12 (1) (2022) 20355.
- [33] M. Chapwanya, A. Matusse, Y. Dumont, On synergistic co-infection in crop diseases. the case of the Maize Lethal Necrosis Disease, *Applied Mathematical Modelling* 90 (2021) 912–942.

- [34] J. Miller, T. M. Burch-Smith, V. V. Ganusov, Mathematical modeling suggests cooperation of plant-infecting viruses, *Viruses* 14 (4) (2022) 741.
- [35] M. Lipsitch, C. Colijn, T. Cohen, W. P. Hanage, C. Fraser, No coexistence for free: neutral null models for multistrain pathogens, *Epidemics* 1 (1) (2009) 2–13.
- [36] S. Alizon, Co-infection and super-infection models in evolutionary epidemiology, *Interface Focus* 3 (6) (2013) 20130031, (**).
- [37] S. Alizon, Parasite co-transmission and the evolutionary epidemiology of virulence, *Evolution* 67 (4) (2013) 921–933, (*).
- [38] S. Bhowmick, K. K. Kasi, J. Gethmann, S. Fischer, F. J. Conraths, I. M. Sokolov, H. H. Lentz, Ticks on the run: A mathematical model of Crimean-Congo Haemorrhagic Fever (CCHF) – key factors for transmission, *Epidemiologia* 3 (1) (2022) 116–134, (*).
- [39] J.-P. Gonzalez, J.-L. Camicas, J.-P. Cornet, O. Faye, M. Wilson, Sexual and transovarian transmission of Crimean-Congo haemorrhagic fever virus in *Hyalomma truncatum* ticks, *Research in Virology* 143 (1992) 23–28.
- [40] A. Matser, N. Hartemink, H. Heesterbeek, A. Galvani, S. Davis, Elasticity analysis in epidemiology: an application to tick-borne infections, *Ecology Letters* 12 (12) (2009) 1298–1305.
- [41] A. Gargili, A. Estrada-Peña, J. R. Spengler, A. Lukashev, P. A. Nuttall, D. A. Bente, The role of ticks in the maintenance and transmission of Crimean-Congo hemorrhagic fever virus: A review of published field and laboratory studies, *Antiviral research* 144 (2017) 93–119.
- [42] J. R. Spengler, É. Bergeron, C. F. Spiropoulou, Crimean-Congo hemorrhagic fever and expansion from endemic regions, *Current Opinion in Virology* 34 (2019) 70–78.
- [43] J.-P. Gonzalez, J.-L. Camicas, J.-P. Cornet, M. Wilson, Biological and clinical responses of West African sheep to Crimean-Congo haemorrhagic fever virus experimental infection, *Research in Virology* 149 (6) (1998) 445–455.

- [44] T. Hoch, E. Breton, Z. Vatansever, Dynamic modeling of Crimean-Congo hemorrhagic fever virus (cchfv) spread to test control strategies, *Journal of Medical Entomology* 55 (5) (2018) 1124–1132, (*).
- [45] P. Van den Driessche, J. Watmough, Reproduction numbers and sub-threshold endemic equilibria for compartmental models of disease transmission, *Mathematical Biosciences* 180 (1-2) (2002) 29–48.
- [46] O. Diekmann, J. A. P. Heesterbeek, J. A. Metz, On the definition and the computation of the basic reproduction ratio R_0 in models for infectious diseases in heterogeneous populations, *Journal of Mathematical Biology* 28 (4) (1990) 365–382.
- [47] J. Heesterbeek, M. Roberts, The type-reproduction number T in models for infectious disease control, *Mathematical Biosciences* 206 (1) (2007) 3–10.
- [48] S. P. Johnstone-Robertson, M. A. Diuk-Wasser, S. A. Davis, Incorporating tick feeding behaviour into R_0 for tick-borne pathogens, *Theoretical Population Biology* 131 (2020) 25–37, (**).
- [49] T. E. Sorvillo, S. E. Rodriguez, P. Hudson, M. Carey, L. L. Rodriguez, C. F. Spiropoulou, B. H. Bird, J. R. Spengler, D. A. Bente, Towards a sustainable one health approach to Crimean-Congo hemorrhagic fever prevention: Focus areas and gaps in knowledge, *Tropical Medicine and Infectious Disease* 5 (3) (2020) 113.
- [50] S. C. Mpeshe, H. Haario, J. M. Tchuente, A mathematical model of Rift Valley fever with human host, *Acta Biotheoretica* 59 (3) (2011) 231–250.
- [51] G. Belluccini, Stochastic models of cell population dynamics and tick-borne virus transmission, Ph.D. thesis, University of Leeds, (*) (2023).
- [52] M. Maliyoni, H. D. Gaff, K. S. Govinder, F. Chirove, Multipatch stochastic epidemic model for the dynamics of a tick-borne disease, *Frontiers in Applied Mathematics and Statistics* 9 (2023) 1122410, (*).
- [53] J. R. Artalejo, M. J. Lopez-Herrero, On the exact measure of disease spread in stochastic epidemic models, *Bulletin of Mathematical Biology* 75 (2013) 1031–1050.

- [54] Y. Yuan, L. J. Allen, Stochastic models for virus and immune system dynamics, *Mathematical Biosciences* 234 (2) (2011) 84–94.
- [55] D. C.-D. Lin, S.-C. Weng, P.-N. Tsao, J. J. H. Chu, S.-H. Shiao, Co-infection of dengue and Zika viruses mutually enhances viral replication in the mosquito *Aedes aegypti*, *Parasites & Vectors* 16 (1) (2023) 1–14, (*).
- [56] G. Cardano, T. R. Witmer, O. Ore, *The rules of algebra: Ars Magna*, Vol. 685, Courier Corporation, 2007.
- [57] D. Zwillinger, *CRC standard mathematical tables and formulas*, CRC press, 2018.